JCI insight

Stem cell and niche regulation in human short bowel syndrome

Vered Gazit, … , Marc S. Levin, Deborah C. Rubin

JCI Insight. 2020. https://doi.org/10.1172/jci.insight.137905.

Research In-Press Preview Gastroenterology

Graphical abstract

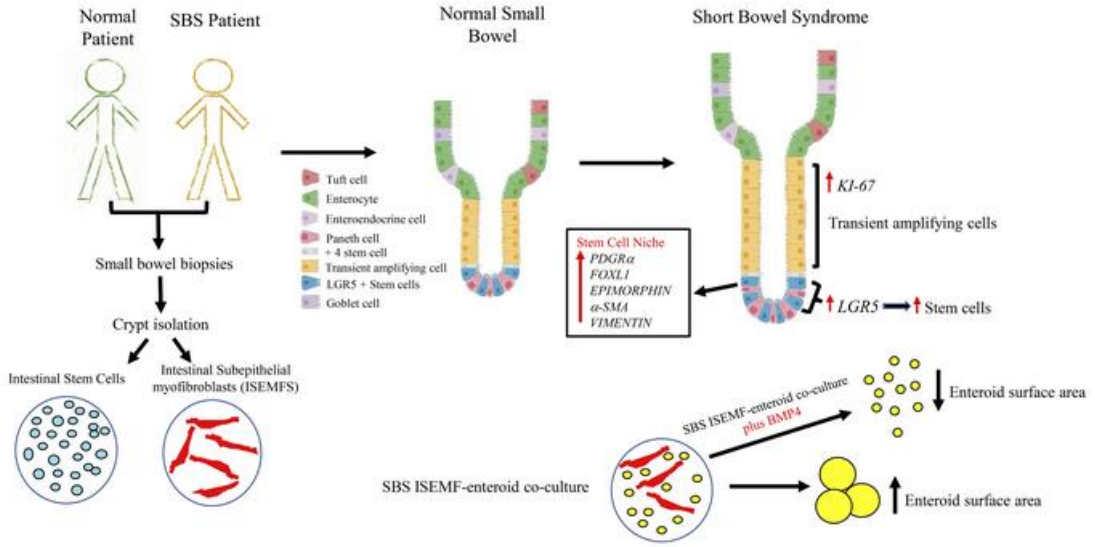

Find the latest version:

https://jci.me/137905/pdf

Stem Cell and Niche Regulation in Human Short bowel Syndrome

Vered A. Gazit[1], Elzbieta A. Swietlicki[1], Miranda U. Liang[1], Adam Surti[1], Raechel McDaniel[1], Mackenzie Geisman[1], David M. Alvarado[1], Matthew A. Ciorba[1], Grant Bochicchio[2], Obeid Ilahi[2], John Kirby[2], William J. Symons,[2,3] Nicholas O. Davidson[1,4], Marc S. Levin[1,5], and Deborah C. Rubin[1,4]

Affiliations: [1]Division of Gastroenterology, Washington University School of Medicine; [2]Department of Surgery, Washington University School of Medicine; [4]Department of Developmental Biology, Washington University School of Medicine; [5]Veterans Affairs Medical Center, St. Louis MO.

Corresponding Author:
Deborah C. Rubin, M.D., AGAF
Division of Gastroenterology
Washington University School of Medicine
660 South Euclid Ave. Box 8124
St. Louis, MO 63110
drubin@wustl.edu
Phone: 314 362 8935
FAX: 314 362 8959

[3] Present address:
William J. Symons, MD
Dept. of Surgery
Stamford Health Medical Group
Stamford, CT.

Conflict of interest statement: The authors have declared that no conflict of interest exists.

Abstract:

Loss of functional small bowel surface area following surgical resection for disorders such as Crohn's disease, intestinal ischemic injury, radiation enteritis, and in children, necrotizing enterocolitis, atresia and gastroschisis, may result in short bowel syndrome, with attendant high morbidity, mortality and health care costs in the U.S. Following resection, the remaining small bowel epithelium mounts an adaptive response resulting in increased crypt cell proliferation, increased villus height, crypt depth and enhanced nutrient and electrolyte absorption. Although these morphologic and functional changes are well-described in animal models, the adaptive response in humans is less well understood, and clinically the response is unpredictable and often inadequate. Here we address the hypotheses that human intestinal stem cell populations are expanded and the stem cell niche is regulated following massive gut resection in short bowel syndrome. We use intestinal enteroid cultures from SBS patients to show that the magnitude and phenotype of the adaptive stem cell response is regulated by stromal niche cells including intestinal subepithelial myofibroblasts, which are activated by intestinal resection to enhance epithelial stem and proliferative cell responses. Our data suggest that myofibroblast regulation of bone morphogenetic protein signaling pathways plays a role in the gut adaptive response post resection.

Introduction

Loss of functional small bowel surface area following surgical resection for Crohn's disease, ischemic injury, radiation enteritis, trauma, or malignancy may result in short bowel syndrome (SBS), an important cause of morbidity, mortality and health care costs in the U.S (1). Necrotizing enterocolitis and congenital disorders such as atresia and gastroschisis are the major causes of SBS in children. Following resection, the remaining small bowel epithelium mounts an adaptive response resulting in increased crypt cell proliferation, increased villus height, crypt depth and enhanced nutrient and electrolyte absorption (2). The functional and morphometric adaptive response is best-described in animal models. In humans, this response is influenced by remnant small bowel length, the presence or absence of a colon, and underlying disease activity, yet even accounting for these factors, the response may be unpredictable and inadequate (1, 3). Even with an accurate assessment of remnant small bowel length, it may require from 2-5 years to determine which patients will wean off parenteral (intravenous) nutrition (4).

There are few studies of gut adaptation in human SBS and these are inconclusive due to limited numbers of patients (5, 6). Patients with SBS have been reported to have an increase (7, 8) or no change (9, 10) (11) in crypt cell proliferation rates and morphologic adaptation post resection (reviewed in (6)). These studies, which are clinically heterogeneous, include infants (7), jejunoileal bypass patients (8), and studies of colon adaptation (9). Only two studies have focused on the small bowel (10, 11). These report modest numbers of patients (11) with limited data on crypt-villus morphometrics (10), and no analysis of stem cell and crypt proliferative responses. Furthermore, treatments for SBS are for the most part non-specific and are directed towards symptomatic diarrhea control. Only one therapy has been developed that is specific to SBS, teduglutide. This glucagon-like peptide 2 analog has multiple pro-adaptive effects, including increasing crypt cell proliferation, crypt depth and villus height. Teduglutide is effective in reducing PN requirements in properly selected patients, of whom a subset may completely wean from PN. Yet others remain at least partially PN dependent, are ineligible for this medication, or develop side effects (12), thus additional therapies are needed. Critical interactions between luminal and host signaling pathways that modulate the stem cell/proliferative and functional adaptive response have yet to be elucidated. Accordingly, understanding the signaling pathways that

modulate intestinal stem cell interactions with the local (niche) environment following small bowel resection is a critical unmet need**.**

Mesenchymal cells play an important role in the gut stem cell niche, in health and in injury and disease (13, 14). We and others have shown that intestinal subepithelial myofibroblasts (ISEMFs) have stem cell niche activity in mouse gut and support stem cell survival and growth of co-cultured epithelial stem cell derived enteroids (15-17) . Our previous studies suggest an important role for epimorphin, a syntaxin that regulates growth factor and cytokine secretion from ISEMFs (15-17). Also cell populations in mice marked by FOXL1 (18, 19), PDGFRα (20), Gremlin1 (21), GLI1 (22, 23) and CD34/GP38 (24) have significant niche activity and are required for stem cell proliferation. Single cell RNAseq analysis of colon biopsies from ulcerative colitis patients have revealed novel mesenchymal populations with stem cell niche activity that may serve as targets for therapy (13). However the characterization and role of these stromal populations in human gut and in SBS is unknown.

Here we address the hypotheses that a subset of intestinal stem cells are expanded and that the stem cell niche is regulated following massive gut resection in human SBS. The magnitude and phenotype of the adaptive stem cell response is regulated by stromal niche cells including ISEMFs that are activated by intestinal resection to enhance epithelial stem and proliferative cell responses. Our data suggest that ISEMF regulation of bone morphogenetic protein signaling pathways plays a role in the gut adaptive response following small bowel resection.

Results

Human SBS stem cell isolation:

Patient Population: To examine the effects of massive small bowel resection and resulting SBS on small intestinal stem cell populations and the stem cell niche in humans, we collected small bowel biopsies from 17 patients with SBS and from 24 control subjects, obtained as part of routine clinical care (see Methods). The demographics of the SBS population including age, gender, race and etiology of SBS, and diet history (oral vs parenteral nutrition) are summarized in Table 1 and details are reported in Supplemental Table 1. SBS patients included those fed an oral diet only or fed partially or completely with parenteral nutrition (PN) for various times post-resection. There were 9 patients with >50% colon remaining in continuity, 1 patient with a sigmoid colostomy who had <50% colon remaining, and 7 patients with small bowel ostomies. SBS resulted from Crohn's disease (n=6), radiation enteritis (n=3), ischemia (n=4), fistula (n=1), trauma (n=1) and adhesions (n=2). There were 7 males and 10 females with an average age of 59.6 years; 6 patients were fed with oral nutrition only.

Transit amplifying cells and *LGR5*+ intestinal stem cells are increased in patients with SBS.

Total RNA was isolated from small bowel biopsies and expression of transit amplifying proliferative crypt cell gene markers (*KI67* and *CD44*) and stem cell gene markers (*LGR5*, *SOX9* and *BMI1*) was analyzed by qRT-PCR.

Expression of *KI67* and *CD44* mRNA was significantly increased in SBS compared to normal patient biopsies (Fig. 1A), consistent with increased crypt transit amplifying cell proliferation (a hallmark of mouse models of adaptation following resection (25, 26)). EGFR/RAS/MAPK signaling is a major driver of proliferation that promotes the exit of stem cells into the transit amplifying cell population (27). Therefore we measured EGFR mRNA expression by qRT-PCR and observed a significant increase in EGFR expression in SBS (Fig. 1A). To correlate mRNA with cell-specific expression, we analyzed KI67 expression by immunohistochemical analysis (Figs. 1B-E). SBS biopsies showed lengthening of the crypts compared to normal biopsies, and immunohistochemistry showed increased crypt expression in the transit-amplifying population associated with increased crypt depth in SBS patients (Fig. 1B-E).

To determine whether the increase in transit amplifying cell proliferation also reflected an expansion of stem cell populations, we examined expression of *LGR5*, the definitive marker of the rapidly dividing gut crypt base stem cell population that replenishes epithelial cells lost by daily cell turnover (Fig. 1F). We observed a significant increase in *LGR5* expression in SBS biopsies compared to normal patients.

In contrast, expression of the quiescent +4 stem cell population marker, *SOX9* (28), was unchanged in SBS, and expression of *BMI1,* a putative marker of the quiescent +4 stem cell population and of enteroendocrine cells that de-differentiate when injured to become stem cells (29), was not significantly increased (Fig. 1F).

We next examined cell-specific *LGR5* expression in SBS biopsies by in situ hybridization analysis using RNAscope fluorescent assays. As expected, *LGR5* mRNA was located at the base of the crypts (Fig. 2A). Quantitation of cellular *LGR5* mRNA expression by Image J analysis showed significantly increased expression in SBS (Fig. 2B; p=0.034).

Increased stem cell activity in human SBS:

To determine whether the increase in *LGR5* expression was reflected by a functional increase in stem cell activity, we performed stem cell initiated enteroid formation assays and compared the ability of SBS compared to normal patient stem cells to form enteroids (Fig. 3). Crypts were isolated from SBS and normal intestinal biopsies, dissociated and cultured to produce stem cell derived enteroids. These were passaged twice, released from Matrigel and frozen. To perform stem cell enteroid initiation assays, stem cells from SBS (n=7) and normal patients (n=12) were obtained from frozen stem cell stocks. Single stem cells ~~w~~ere plated in Matrigel and the number of surviving enteroids were imaged and counted on day 7 post plating.

SBS patients had a significant increase in the number of stem cell-derived enteroids compared to normal subjects (Fig. 3A,C), providing a functional correlation for the observation that LGR5 mRNA levels were increased in SBS (Figs. 1,2). These results also indicate that even after passaging and freezing, SBS stem cells retained the observed *in vivo* phenotype for expansion compared to normal stem cells. Enteroid size (cross-sectional area), which reflects growth of each surviving stem cell derived colony, was unchanged in SBS compared to normal subjects (Fig. 3B).

WNT ligand and target gene expression in SBS:

LGR5+ stem cell proliferation and commitment to specific differentiation pathways are regulated by WNT, BMP and NOTCH signaling (30), contributing to autocrine and niche regulation of stem cell maintenance and expansion. To begin to assess WNT signaling activity in SBS, we examined expression of downstream WNT target genes including *AXIN2*, *cyclin D1*, *C-MYC*, WNT signaling pathway components including *DKK1* and *β-CATENIN*, and WNT agonists and ligands by qRT-PCR. Although LGR5+ cell populations were expanded, there was no change in *WNT* target gene expression, including *cyclin D1*, *C-MYC, DKK1* or *β-CATENIN* and *AXIN2* expression showed a trend to be decreased in SBS compared to normal biopsies (Fig. 4A p=0.054). In contrast, expression of LGR4-6 receptor ligands/WNT agonists *Rspondin1* and *Rspondin2,* was significantly increased in SBS vs. normal biopsies (Fig. 3B). *Rspondin3* expression was unchanged. Rspondin1 is expressed in epithelial and mesenchymal cells, Rspondin2 and Rspondin3 are expressed predominantly in mesenchyme (31) (32). MRNA expression of the mesenchymal *WNT* ligand *WNT5a* was also increased.

BMP signaling pathways are regulated in human SBS:

Increased ligand expression without concomitant increased WNT signaling activity suggested that the SBS mesenchyme generates a stromal niche adaptive response following resection to facilitate stem cell expansion, but WNT signaling activity may be inhibited by other counter-regulatory pathways such as the bone morphogenetic protein (BMP) pathway. BMP signaling plays a role in the small intestinal stem cell niche, regulating crypt cell proliferation and epithelial cell differentiation (30). BMP signaling activity is lowest at the base of the crypt, due to enriched mesenchymal expression of BMP inhibitors including noggin, gremlin and chordin (33, 34), and increases along the crypt-villus axis as cells exit the crypt and differentiate during migration onto the villus, inhibiting stem and crypt cell proliferation and promoting epithelial cell differentiation.

We quantified mRNA expression of *BMP4*, *BMP2* and *BMP7* and *BMP* inhibitors *noggin*, *gremlin*, *chordin* and *follistatin*. Expression of *BMP4* mRNA, which inhibits stem and crypt cell proliferation and promotes epithelial differentiation, was significantly increased in SBS intestine (Fig. 5A). *BMP2* and *BMP7* showed no change (data not shown). Conversely expression of BMP inhibitors *gremlin1*, *noggin*, *chordin* and follistatin were unchanged in SBS vs. controls.

To further examine whether BMP signaling activity is regulated in SBS, we next examined expression of P-SMAD1,5,8, the major downstream target of BMP signaling by immunoblot. We found that SBS biopsies had increased P-SMAD1,5,8 expression compared to normal gut, which showed low basal levels of P-SMAD1,5,8 expression (Fig. 5B). Thus BMP signaling activity appears to be increased overall in SBS mucosa.

Mesenchymal stem cell niche populations in SBS

To further explore the cellular basis for the increase in mesenchymal WNT ligand, WNT agonist (Rspondins) and BMP4 expression, we examined the adaptive SBS response of gut mesenchymal (stromal) cell populations that have stem cell niche activity (13, 18-20, 22, 24, 27) by cell marker expression analyses using qRT-PCR. Gut mesenchymal populations include ISEMFs which are smooth muscle α-ACTIN (SMA)-positive, vimentin-positive, desmin-negative cells which express epimorphin, a myofibroblast protein that regulates growth factor secretion (15, 16) and FOXL1+ telocytes, which also have been shown to play a role in the stem cell niche in mouse models and in human inflammatory bowel disease (13). Also CD34/GP38+ cells (24) and SMA-/ PDGFRα+/Rspondin3+ cells have been described in mouse intestine (20). These cells all express PDGFRα (27) and are the source of WNT ligands and Rspondins, including WNT2b, WNT4, WNT5a and Rspondin1, 2 and 3, and BMPs (27).

Expression of *vimentin*, *SMA* and *epimorphin* mRNA was significantly increased in SBS biopsies by qRT-PCR (Fig. 6A) consistent with expansion and/or activation of myofibroblasts, which express mesenchymal WNTs and Rspondin1, 2 and 3. In addition, *FOXL1* and *PDGFRα* mRNA expression was increased in SBS vs control small bowel (Fig. 6); in contrast, *CD34* expression was reduced and expression of *GP38* and R-spondin3 (as per Fig. 4B) was unchanged. Therefore, subpopulations of some, but not all, PDGFRα+ cells respond to loss of functional small bowel surface area, suggesting cell-specific adaptation.

To examine the cellular basis for the increased expression of multiple mesenchymal cell markers, we performed immunohistochemical analysis to detect PDGFRα+ cells. We noted a significant increase in PDGFRα+ cells in the villus cores of SBS compared to control biopsies (Fig. 6B,C).

Outlier and subgroup analyses

Outlier analyses followed by additional subgroup analyses were performed for all the data reported in Figure 1 and Figures 4-6 to determine whether outliers have a unique clinical phenotype, as per Methods. We found no

association of outliers with the presence or absence of a colon in continuity, age, gender, intestinal location (duodenum, jejunum or ileum) or oral feeding vs. parenteral nutrition.

SBS ISEMFs increase growth of co-cultured SBS enteroids

To further explore mesenchymal cell-specific effects on stem cell proliferation and the stem cell niche, we isolated human ISEMFs from SBS and normal control patient biopsies. ISEMFs were chosen for further study because these cells expressed activation markers in SBS compared to normal intestine, (*α-SMA*; Fig. 6). ISEMFs were co-cultured with SBS and normal stem cells, and the number and size (surface area) of surviving enteroids were measured after 7 days in co-culture (Fig. 7). We found that SBS enteroid size increased when co-cultured with SBS ISEMFs compared to co-cultures with normal patient ISEMFs (Fig. 7A,C). In contrast, there was no effect on the size of normal enteroids when co-cultured with SBS compared to normal ISEMFs, suggesting a specific interaction between SBS ISEMFS with SBS enteroids.

The number of stem cell derived enteroids was significantly lower in normal enteroid-SBS ISEMF co-cultures compared to normal enteroid-normal ISEMF co-cultures (Fig. 7B). In contrast, there was no change in SBS enteroid cell count when co-cultured with normal vs SBS ISEMFs, again suggesting that SBS enteroids have cell autonomous changes that alter their response to co-culture with ISEMFs.

To elucidate the mechanisms underlying the effect of SBS ISEMFs on SBS enteroid growth, we examined markers of myofibroblast activation and function in isolated ISEMFs (Fig. 8A,B). SBS ISEMFs exhibited increased SMA mRNA expression compared to normal ISEMFs. In contrast, *epimorphin* mRNA expression was decreased in SBS compared to normal patient ISEMFS, consistent with observations in mouse intestinal adaptation post resection (35) and with studies which showed that *epimorphin* deletion in mouse gut results in enhanced crypt cell proliferation (36) and increased enteroid growth in *Epim*$^{-/-}$ ISEMF-enteroid co-cultures (15). Expression of other mesenchymal markers such as *FOXL1* and *PDGFRα* were unchanged in SBS vs normal ISEMFs.

BMPS are expressed and secreted by ISEMFs; therefore we examined SBS and normal myofibroblast expression of members of the BMP signaling pathway, including *BMP4* and inhibitors *chordin* and *noggin*. In contrast to what we observed in SBS biopsies which reflects an average increase in *BMP4* expression across all cell types, (Fig. 5), we observed a significant decrease in *BMP4* mRNA expression in SBS ISEMFs

compared to controls (Fig. 8C), without change in *noggin* or *chordin* mRNA expression, suggesting ISEMF cell-specific regulation of BMP expression.

To determine if reduced BMP4 expression in and secretion from SBS ISEMFs could explain the growth-inducing effect of these cells on SBS enteroids, we co-cultured SBS enteroids with SBS ISEMFs, without the BMP inhibitor noggin and with recombinant BMP4 (25 ng/ml; Fig. 9) or vehicle. Addition of BMP4 reversed the SBS ISEMF-induced increase in enteroid size (Fig. 9A), but had no effect on the size of normal enteroids when co-cultured with normal or SBS ISEMFs (Fig. 9B). Thus it appears that BMP signaling is inhibited in SBS ISEMF-SBS enteroid co-cultures, resulting in increased growth. In contrast, the reduction in the number of stem cell derived normal enteroids when co-cultured with SBS vs normal ISEMFs (Fig. 7B), was not reversed by addition of BMP4 (Fig. 9C). Thus reduced BMP signaling resulted in an increase in SBS but not normal enteroid growth, but this signaling pathway does not direct the reduction in enteroid number, suggesting regulation of this response by other factors/pathways.

Discussion:

Here we report that massive intestinal resection regulates stem and stromal niche cell populations in the residual gut in humans with SBS. We have analyzed small bowel biopsies as well as *in vitro* enteroid and stromal ISEMF cell culture models to begin to elucidate underlying mechanisms for the human adaptive response and to identify potential novel targets for therapy. Our study is unique in that we have obtained mucosal small bowel biopsies from a large cohort of SBS patients, a critically important step forward since this is a clinically heterogeneous population (37). Prior studies (5, 7-11) of the cellular and morphometric features of the human gut adaptive response have been limited by small sample size.

We found that the adaptive SBS intestine has an expanded stem cell population, as shown by stem cell initiated enteroid formation assays (Fig. 3) and by increased expression of *LGR5* mRNA (Figs. 1,2), the intestinal stem cell marker of the rapidly cycling crypt base stem cell that is responsible for daily renewal of the small bowel epithelium (38). Our analysis of the SBS mesenchyme shows a selective expansion of a subset of stromal cells with putative roles in regulating the stem cell niche. Our data indicate that there is a specific stromal cell adaptive response rather than just a general increase in all stromal cells because we showed that cells expressing CD34/GP38 (Fig. 6), which have niche activity in mice (22, 24), are not expanded in intestinal biopsies from human subjects with SBS. We further show that ISEMFs induce growth of co-cultured stem cell-initiated enteroids via reduced BMP signaling, but only in the setting of SBS.

We found that slower cycling “reserve” +4 stem cell populations marked by SOX9 (28) and BMI1 (39) are not expanded in SBS intestine, findings that contrast with the expansion of LGR5+ cells. The biopsies collected in this study were from patients who had SBS for a duration of 6 months up to >10 years. It is possible that the reserve stem cell population responds to resection at earlier times after surgery, e.g. in the first few months post-resection. These biopsies are more difficult to obtain given the severity of illness early after resection, but are required to specify which stem cell population(s) are first mobilized following extensive resection.

Although *LGR5* mRNA expression was significantly increased in small bowel biopsies from SBS vs. control patients and stem-cell initiated enteroid formation was greater in SBS patients compared to controls (Figs. 1-3), we observed patient-to-patient variability for all the analyses. Due to the limited number of samples, we were unable to subdivide our groups to analyze adaptive gene expression in biopsies from patients who had a

colon in continuity vs. those with ileostomy or jejunostomy, or from patients who were on oral vs parenteral feeding, etc. We also pooled duodenal, jejunal and ileal biopsies from SBS patients and normal subjects, while recognizing that geographic differentiation could affect the results. However we focused on analyzing expression of genes that have similar, general functions throughout the GI tract (proliferation, stem cell function, etc.). Also we performed outlier analyses of all the biopsy-derived mRNA expression data, followed by additional subgroup analysis to see if the outliers have a unique clinical phenotype. Outlier analysis did not reveal a correlation with age, gender, presence or absence of colon, location of biopsy (duodenum, jejunum or ileum) or oral vs parenteral feeding (i.e. on vs off TPN). This variability also did not appear to result from differences in the size or mucosal/submucosal depth of the biopsies, because there was no consistent pattern of very high or very low expression levels of multiple genes in an individual patient. Similarly, increased expression of epithelial and stromal marker genes in SBS was not simply due to adaptive crypt and villus hyperplasia, because multiple markers of the proliferative, differentiating and stromal epithelium showed no difference in expression levels in SBS vs normal gut (e.g. *SOX9*, *GP38*, *gremlin*, β-*CATENIN*, etc.). However, firm conclusions about whether there is a significant association with specific demographic features or with disease process (e.g. Crohn's disease, ischemia, adhesions, etc.) will require analysis of larger numbers of samples per group.

SBS-induced stem cell expansion and increased stem cell function measured by assays of stem cell derived enteroid initiation (Fig. 3) was preserved in these cells following several passages and in assays which used stem cells that had been passaged and were frozen for storage. This phenotypic preservation with passaging and after removal of both luminal and submucosal signals suggests a cell–autonomous mechanism, and specifically, epigenetic modulation has been shown to be responsible for preservation of other phenotypic changes. For example, others have shown that regional small bowel epithelial identity along the horizontal axis (e.g. from duodenum to ileum) is recapitulated in enteroids due to preservation of intrinsic DNA methylation patterns with passaging and in long term culture (40). DNA methylation profiles were preserved independent of the cellular environment in adult and pediatric organoids, but interestingly fetal organoids showed *in vitro* maturation, with changes in DNA methylation in culture. Also, disease-specific changes in methylation were identified in organoids derived from a patient with gastric heterotopia which were also preserved in passaging.

Similarly, changes in Crohn's disease and ulcerative colitis patient enteroid gene expression patterns compared to normal enteroids are also preserved after passaging, likely due to retained epigenetic changes (41, 42). Similar epigenetic mechanisms are likely to be operative in the setting of SBS.

Bone morphogenetic protein (BMP) signaling activity is regulated along the crypt-villus axis. BMP inhibitors are produced by pericryptal stromal cells in humans (33). Inhibition of BMP signaling activity is highest at the crypt base where WNT signaling activity is highest, promoting stem cell expansion. BMP4 is expressed in mesenchymal cells adjacent to intestinal stem cells and noggin is expressed in submucosal cells adjacent to the crypt bottom in mice (43). Stem cell dependence on BMP inhibition is well established, as illustrated by the requirement for exogenous noggin for successful growth of stem cell-derived enteroid cultures *in vitro* (44). BMP signaling activity increases above the crypt base, from the mid-crypt and higher along the crypt–villus axis to inhibit crypt cell proliferation in the transit amplifying zone and promote epithelial differentiation, counterbalancing WNT signaling activity (30, 45). Mesenchymal BMP expression and BMP signaling activity increases from mid crypt onto the villus (30) (45). BMPs are expressed by mesenchymal cells including ISEMFs (Fig. 8 and (16, 34)), Foxl1+ telocytes (in mice) (19) and by stromal cells in human colon (BMPS 2,5,7) that have yet to be fully characterized (13). The major small intestinal BMPs are BMP2, BMP4 and BMP7 (45). In mice, BMP4 and BMP inhibitors are expressed by mesenchymal cells whereas BMP2 is expressed by the epithelium (33). In humans, single cell RNAseq showed that *BMP2* and *BMP5* are expressed in a unique subset of colon stromal cells (13); BMP2 and 4 are expressed in human small bowel in epithelium and in stroma, respectively (https://www.proteinatlas.org/search/bone+morphogenetic+protein), but cell-specific expression patterns of other Bmps and inhibitors in human small intestine have not yet been elucidated.

Our analysis of SBS vs. normal patient biopsies shows an increase in BMP4 mRNA and increased P-SMAD1,5,8, consistent with increased BMP4 signaling overall, which is active on the villus and is required for epithelial differentiation. Yet, our analysis of crypt-derived enteroid-specific interactions with ISEMFs suggests a local, crypt specific decrease in BMP signaling (Figs. 8,9). This is consistent with BMP signaling inhibition at the crypt base. We observed that ISEMFs from SBS patients have reduced BMP4 mRNA expression compared to normal ISEMFs (Fig. 8), and incubation of ISEMF-SBS enteroid co-cultures with exogenous

BMP4 reverses the SBS ISEMF-induced increase in enteroid surface area (Fig. 9). Thus the SBS ISEMF stromal cell population responds to resection locally at the crypt, by inhibiting BMP expression, favoring increased crypt cell proliferation.

Co-cultures of SBS ISEMFs vs. normal ISEMFs with SBS stem-cell derived enteroids induced growth (increased surface area) of co-cultured enteroids, but not stem cell expansion; the number of stem cell-initiated enteroids in SBS-ISEMF-SBS enteroid co-cultures compared to normal ISEMF-SBS enteroid co-cultures was not significantly decreased (Fig. 7). Also, comparison of normal enteroid-SBS ISEMF co-cultures with normal enteroid-normal ISEMF co-cultures revealed a significant decrease in the number of stem cell initiated enteroids but no change in surface area/growth. These results suggest that SBS ISEMFs expand the proliferative transit amplifying cell program, resulting in increased enteroid growth in co-culture, but do not have direct effects on the stem cell population. Thus, other stromal cell populations (e.g. FOXL1 telocytes, other PDGFRα+ cells, etc. (13, 19, 20, 27)) or stem cell/epithelial autonomous mechanisms may regulate the observed expansion in SBS (Fig. 3). The observation that co-culture of SBS ISEMFs increases growth of SBS stem cell-derived enteroids but not normal enteroids (Figs. 7,9) suggests resection-induced changes in cell surface growth factor or growth inhibitor receptor expression that are specific to SBS enteroids. Further studies are required to elucidate these mechanisms.

The role of WNT signaling activity in establishing and maintaining stem cell expansion and amplifying population crypt cell proliferation in the human adaptive intestine has not been previously studied. Limited experiments in rodent adaptation following resection show that *Apc*$^{min/+}$ mice have an increased crypt cell proliferative response early after resection (e.g. 72h post resection (46)), yet Wnt signaling doesn't play a role in maintaining this morphometric response (47). Others have shown that Wnt signaling is inactive in the mouse gut transit amplifying cell population although EGFR/RAS/MAPK signaling enhances proliferation of this cell population (27) (48). We found that EGFR expression was significantly increased in SBS biopsies, consistent with a role for this signaling pathway in human SBS. In our present observations of adaptive intestine that has reached a "steady state" following resection, we observed an increase in WNT ligand and agonist expression (*Rspondin 1, 2* and *WNT5a*) without concomitant increased WNT signaling activity (Fig. 4); in fact *AXIN2* mRNA expression showed a trend to be decreased (p=0.054), suggesting WNT signaling

inhibition. These data suggest that the mesenchyme responds to the loss of small bowel surface area by a compensatory increase in WNT and R-spondin ligand expression, but that other counter-regulatory mechanisms are activated to inhibit WNT signaling, possibly to protect from chronic WNT stimulation that could result in tumor formation/carcinogenesis. BMP signaling is likely to be one of these counter-regulatory mechanisms (43). Our results do not exclude the possibility that WNT-driven expansion of LGR5+ stem cells occurred at earlier times post-resection, since our patients have had SBS for 6 months to >10 years.

The effect of myofibroblasts on co-cultured-enteroid growth suggests that examination of other niche cell populations to elucidate effects on stem cell proliferation and expansion could provide novel therapeutic targets for SBS. For example, FOXL1+ cells have been proposed to be critically important niche cells for maintaining a normal crypt; however, these cells are relatively rare, making isolation from human intestine challenging. The current findings point to an emerging role of BMP signaling, but clearly other signals are yet to be identified in the adaptive response.

Methods

Human studies

All human studies were performed following protocols approved by the Washington University School of Medicine's Institutional Review Board, as per IRB #201504100. All studies were conducted according to Declaration of Helsinki principles. Informed consent was obtained for all studies.

Patient population

Patients with SBS (n= 17; Table 1 and Supplemental Table 1) were recruited from the Gastroenterology Clinic (DCR) at Washington University in St. Louis School of Medicine or from Barnes-Jewish Hospital in St. Louis. SBS was defined as a residual small bowel length of ≤200 cm, with or without part or all of the colon in continuity. These included patients with jejuno-ileal anastomosis and ileostomy, jejunostomy, ileo-colonic anastomosis or jejunocolonic anastomosis. As per standard practice, all patients were permitted to ingested oral enteral diets even if receiving intravenous (parenteral) nutrition support.

Control subjects (n=27) were recruited from the Gastrointestinal Endoscopy Lab at Washington University in St. Louis School of Medicine/Barnes-Jewish Hospital, or from the general surgical service. Endoscopy control patients included those who presented for routine colon cancer screening or for routine upper endoscopy for evaluation of esophageal or gastric symptoms but were anticipated to have normal small intestine, which was confirmed during endoscopy. During colonoscopy, the normal terminal ileum was intubated and biopsied. Normal jejunum was obtained from patients undergoing intestinal fistula repair; biopsies were taken from normal adjacent mucosa from surgical intestinal specimens removed for fistula repair.

Human intestinal enteroid isolation and passaging

Duodenal, ileal and jejunal biopsy specimens were obtained from normal patients during routine endoscopy for colon cancer screening, from upper endoscopy for unrelated upper GI symptoms, or from adjacent normal small bowel obtained during fistula repair surgery as detailed above. SBS patient biopsies were obtained during routine clinically indicated endoscopy or from surgical resections performed at Barnes-Jewish Hospital at the Washington University School of Medicine in St. Louis, MO. Patients ingested nothing by mouth for at least 6 hours prior to endoscopy and overnight prior to surgery. Small intestinal enteroids were isolated from biopsy samples as previously described (49). Biopsies were washed with Basic Crypt Media (BCM), consisting of advanced DMEM/F12 with HEPES 10 mM (Sigma D6421), supplemented with 100 U/mL Penicillin/Streptomycin (Sigma), 2 mM Glutamax (Gibco), and 10% FBS (Gibco by Life Technology), cut into small pieces and treated with collagenase Type I (Invitrogen 17100-017,) for 10 minutes at 37˚C. Crypts were collected and resuspended in 10 mL BCM, filtered through a 70 µm strainer (MidSci, Valley Park, MO), and centrifuged at 300g for 5 minutes. Enteroids were suspended in Matrigel (CORNING, 3562237) and plated on 48-well plates. After allowing the crypt-Matrigel suspension to solidify for 10- 15 minutes at 37˚C, cultures were treated with conditioned media (CM) produced from ATCC cell line L-WRN (CRL-3276), which contains Wnt3a (W), Rspondin (R), Noggin (N), and supplemented with 10 µm Y-27632 (p160 ROCK inhibitor, Sigma, Y0503-1MG, dihydrochloride) and 10 µM SB-431542 (TGF-β receptor antagonist, Sigma, SB-431542 hydrate). Culture medium was changed every 3 days. Enteroids were passaged to expand stem cells on day 7 post plating by gentle enzymatic digestion in 0.25% Trypsin/ EDTA (Gibco) for 5 minutes at 37˚C and re-plated in

Matrigel (50 crypts per 15uL of Matrigel) into a 48-well plate and cultured in CM without the addition of 10uM Y-27632. After up to 7 days in culture, stem cells were frozen for storage.

Stem cell enteroid initiation assays

Stem cells were thawed and cultured in Matrigel in CM supplemented withY-27632 and SB 431542, grown for 7 days, and harvested from Matrigel by enzymatic digestion with 0.25% Trypsin/EDTA (Gibco) and with pipetting up and down 20-40 times. Live cells were analyzed by staining with 0.4% Trypan blue dye (Bio-Rad, Hercules, CA) and quantified by TC20 Automated Cell counter (Bio-Rad, Hercules, CA), then replated in Matrigel (50 cells per 15 µl of Matrigel) and grown in CM. Enteroids were imaged with a Zeiss Axiophot microscope with Apotome 2 attachment (Carl Zeiss Inc.) on days 3 and 7 post plating**.**

Stem cell initiation assays and quantitation of enteroid growth

Stem cell initiated enteroid numbers and size were quantified at 3 and 7 days post plating using Cytation 3 plate reader software (BioTek Gen 3.0). The images were analyzed to quantify total number of viable enteroids per well. The total and average cross-sectional area in the optical level of focus was measured. Enteroid viability was defined by the presence of visually sharp borders along their basolateral (anti-luminal) side.

Small bowel biopsies and ISEMF culture and isolation

ISEMFs were isolated from duodenal, jejunal and ileal biopsies, obtained either from normal patients during routine endoscopy for colon cancer screening or from adjacent normal small bowel obtained during fistula repair surgery, and from SBS patients during routine clinically indicated endoscopy or from surgical resections performed at Barnes-Jewish Hospital at the Washington University School of Medicine in St. Louis, MO. Small intestinal biopsies were minced and incubated with 300U/mL collagenase Type 1 and 0.1 mg/mL dispase (Gibco, Carlsbad, CA) for 2 hours at 37°C, washed with ISEMF culture medium (RPMI 1640 media (Gibco, Carlsbad, CA), supplemented with 10% FBS, antimycotic solution (Corning), and 10ug/mL gentamicin (Gibco, Carlsbad, CA)), and plated in 6 well plates at 37°C. After ISEMFs attached and formed colonies, they were subsequently passaged, expanded, and plated in standard myofibroblast cell culture medium. This media consisted of Dulbecco's modified Eagle medium (DMEM)/Glutamax (Invitrogen, Carlsbad, CA) with 10% FBS (Invitrogen), and penicillin/streptomycin (Sigma). The identity and purity of isolated ISEMFs was determined by

immunofluorescence to detect expression of smooth muscle actin (a-SMA) and vimentin, and confirm absence or weak positivity of desmin expression (50). ISEMFs were imaged using a Zeiss Axiovert microscope with Apotome 2 optical sectioning apparatus (Zeiss, Inc.).

Enteroid-myofibroblast co-cultures

ISEMFs from control or SBS patient biopsies were plated into 48-well plates at a density of $1x10^4$ cell/cm^2. Stem cells derived from crypts as above (see **Human intestinal enteroid isolation and passaging)** were frozen for storage and then thawed and cultured in Matrigel in CM supplemented withY-27632 and SB 431542, grown for 3 days, and harvested from Matrigel by enzymatic digestion with 0.25% Trypsin/EDTA (Gibco) and with pipetting up and down 20-40 times, and re-plated in Matrigel (50 live cells per well) onto a 48-well plate, either directly into the well as a monoculture or on top of a pre-confluent (~70 %) monolayer of ISEMFs cultured in CM (containing Wnt3a, R-spondin, noggin, Y-27632 and SB-431542).

Immunoblot analysis

Protein was extracted from phenol-ethanol phase after RNA and DNA precipitation as outlined in the TRIzol (Invitrogen) manufacturer's manual. Briefly, an excess of 100% ethanol was added to the phenol/ethanol phase. Samples were vortexed, incubated for 10 minutes at room temperature following by centrifugation at 12000 g for 10 minutes at 4^0C. Pellets were washed two times in 500 µL 95% ethanol and centrifuged at 7600 g for 5 minutes at 4^0C. After removing ethanol, pellets were air dried for 5 minutes and 40-100 µL of TGH protein lysis buffer containing 25 mM HEPES (pH 7.4), 10% glycerol, 1% Triton X-100, 5mM EDTA supplemented with complete protease inhibitor cocktail (Thermo Scientific –U.S) was added to samples. Samples were concentrated using the Protein- Concentrate (Micro) kit (cat# 2100, EMD Millipore Corporation). Protein content was quantified using Pierce™ BCA Protein Assay kit (Thermo Fisher scientific – U.S), and equal amounts of protein were loaded on Nu-PAGE 4-12% polyacrylamide gradient gel (Life technologies, NY) under reducing conditions, and transferred to nitrocellulose membranes by iBLOT 2 dry blotting system (Life Technologies, NY). Membranes were blocked and probed with antibodies directed against rabbit anti–phospho Smad1/Smad5/Smad8 (Ser463/465) (1:200 Millipore/Sigma, Ab3848-I.), Mouse anti - β-actin (C4) (1:1000 Santa Cruz A1713) was used as a loading control. The optical density of the specific proteins was quantified by using LI-COR imaging system (Odyssey CLx infrared imaging system, LI-COR Biosciences – U.S).

Immunofluorescence analysis of ISEMFs.

ISEMFs were cultured on glass slides, fixed in formalin and processed in situ for immunofluorescence analysis. Staining was performed to identify smooth muscle α-actin (α-SMA: Abcam 5694 rabbit antibody, 1:200), vimentin (Abcam 8978, mouse antibody 1:50), and desmin (Abcam 15200, rabbit antibody, 1:50). Anti-rabbit FITC, anti-mouse FITC, and anti-rabbit Cy3 were each used at 1:200 dilutions (Jackson ImmunoResearch Laboratories). Nuclei were counterstained with Vectashield with DAPI (Vector Labs, Burlingame, CA). Cells were visualized using Nuance microscopy (Nuance™ Multispectral Imaging System).

Immunohistochemical analyses:

Biopsies were fixed in formalin, dehydrated in 70% ethanol and embedded in paraffin. Sections were cut (5 µm) and rehydrated. Heat induced epitope retrieval (Reveal Decloaker 10x, Biocare Medical) was performed for 20 minutes, following by 0.3% peroxidase ((HX0635-3 Millipore, USA), and blocked in Blocking Buffer (Sigma) for 1 hour at room temperature. Specimens were incubated at 4°C overnight with mouse anti- Ki67 (1:400, ab156956, Abcam) or mouse anti- PDGFRα (16AI; 1:100, ab96569, Abcam), then washed and incubated for 30 minutes in a detection reagent (HRP-Polymer, Biocare medical), and developed with diaminobenzidine (DAB; Betazid DAB, Biocare Medical). Sections were counterstained with hematoxylin, and visualized and photographed using an Olympus BX43 microscope (Olympus Life Science, USA).

PDGFRα quantification: The number of PDGFRα+ cells that were subjacent to the villi or to the crypts were quantified. To correct for differences in villus length and crypt depth, the number of positive cells was counted in a rectangular box of fixed area (230 micronX165 micron) which was overlaid onto photomicrographs of the villi and crypts of each biopsy examined. Only intact villi and crypts on each histologic section were analyzed. *p= 0.031 by Student's t test.

In situ hybridization analyses and quantitation:

A target-specific oligonucleotide (ZZ) probe for Lgr5 was designed (Hs-LGR5-C3 (#311021-C3; RNAScope Advanced Cell Diagnostics, Newark, CA.). Multiplexed Fluorescent reagent kit v2-Hs (# 323135, Advanced

Cell Diagnostics) was used as per the manufacturer's protocol. Formalin-fixed paraffin-embedded tissue blocks were sectioned at 4 µm, mounted on slides (ColorView™ Adhesion Slides StatLab, CA.) Slides were pretreated with sequential deparaffinization, hydrogen peroxide, target retrieval, and protease plus digestion, followed by Lgr5 probe hybridization, signal amplification, and detection. Probe hybridization was achieved by incubation mRNA target probes for 2 h at 40°C using a HybEZ oven (Advanced Cell Diagnostics). The signal was amplified by subsequent incubation of Amp-1, Amp-2, Amp-3, HRP Signal and Opal Dye (Akoya Biosciences, CA) /TSA, two drops each for 30, 30, 15, and 30 min respectively at 40°C using the HybEZ oven. Nucleic acids were stained using DAPI, (Advanced Cell Diagnostics, United States), and coverslips were mounted with Prolong Gold Antifade Mountant (Thermo Fisher, United States). The 3-plex negative control probe [ACD, #320871] was applied to separate histologic sections processed in the same manner as those that received the *Lgr5* probe. Slides were visualized under fluorescence microscopy (Zeiss Axiovert microscope with Apotome 2 optical sectioning apparatus (Zeiss, Inc.). To analyze the number of Hs-LGR5 molecules per cell in each SBS and normal small bowel biopsy, Lgr5+ signals were quantified in each positive cell using ImageJ.

Quantitative RT-PCR

RNA was isolated from small bowel biopsies using TRIzol (Invitrogen) reagent according to the manufacturer's instruction, and extracted from ISEMFs using Nucleospin RNA kit (Invitrogen, Carlsbad, CA). Quantification of RNA was performed using 260/280 nm by NanoDrop 2000 (Thermo Fisher Scientist –U.S). Complementary DNA was generated from 1 µg/µl of RNA with Superscript II RT cDNA Synthesis kit (Invitrogen, Carlsbad, CA), which amplified by PCR – 2720 Thermal Cycler (Applied bioscience, Carlsbad, CA). Gene expression was determined by Step One Plus System (Applied Biosystems, Carlsbad, CA) using Fast Cyber Green Master Mix (Applied Biosystems by Thermo Fisher Scientific) for all PCR. Primers used are listed in Table 2**.** Cycle threshold values were normalized to 18s mRNA levels. The fold induction was determined by the ddCt method (51).

BMP 4 effects on enteroids and enteroid-ISEMF co-cultures

Stem cells were removed from frozen storage and incubated in enteroid CM media with Wnt3a, R-spondin, SB-431542 and Y-27632, with or without noggin. Media was changed 3 days post-plating. Imaging and quantitation of surface area and cell count were performed at 3 days post-plating. ISEMF-enteroid co cultures were incubated in CM media as above, with or without Bmp4 (25 ng/ml; recombinant Human BMP4, 314-BP: R&D), but without noggin. Co-cultured enteroids were analyzed for size (surface area) and cell count at 3 days post-plating.

Statistical analyses

Data comparing mRNA expression and enteroid size and cell count from normal patient and SBS biopsies or from ISEMFs and enteroids were calculated as the mean ± standard error of measurement. Statistical significance was analyzed by two-tailed Student's *t* test (GraphPad, Prism 8) comparing normal to SBS samples. *P* values less than or equal to 0.05 were considered significant, and p values are reported in each figure legend.

Outlier values were determined using the rule that defines an outlier as a value larger than 1.5 times the interquartile range from the 75th percentile or smaller than 1.5 times the interquartile range from the 25th percentile. The subject with at least one outlier in the gene group was defined as an outlier. The association between outlier distribution and demographic variables was examined using two-sample t-test for continuous demographic variables and Chi-square test for categorical demographic variables.

Human studies approval

All human studies reported in this manuscript were approved by the Institutional Review Board of Washington University in St. Louis, as indicated in human studies protocol IRB# 201504100. Written informed consent was received from participants prior to inclusion in the study.

Author Contributions

Vered A. Gazit: Designed research studies, performed experiments, analyzed data, contributed to writing manuscript.

Elzbieta A. Swietlicki: Designed research studies, performed experiments, analyzed data.

Miranda Liang: Performed experiments and analyzed data

Adam Surti: Performed experiments and analyzed data

Raechel McDaniel: Performed experiments and analyzed data

Mackenzie Geisman: Performed experiments and analyzed data

David Alvarado: Provided reagents, contributed to designing research studies

Matthew Ciorba: Provided reagents

Grant Bochicchio: Provided reagents

Obeid Ilahi: Provided reagents

John Kirby: Provided reagents

William J Symons: Provided reagents

Nicholas O. Davidson: Experimental design, writing manuscript

Marc S. Levin: Experimental design, writing manuscript

Deborah C. Rubin: Experimental design, data collection, data analysis, writing manuscript.

Acknowledgments

These studies were funded by NIH NIDDK R01 DK106382 (Rubin, Levin), R01 DK112378 (Rubin, Davidson and Levin) and P30 DK052574 (Washington University DDRCC AITAC and Biobank Cores). The authors thank Kymberli May, Lauren Cronk and Sheila Wood of the Advanced Imaging and Tissue Analysis Core of the DDRCC for their expertise and help with our immunohistochemical studies. Graphical abstract was created with BioRender.com.

References

1. Buchman AL. Short-bowel syndrome. *Clinical Gastroenterol Hepatol:*2005;3(11):1066-70.
2. Levin MS and Rubin DC. In: Langnas A.N. GO, Quigley E.M.M. and Tappenden K.A. ed. *Intestinal Failure: Diagnosis Management and Transplantation*. Blackwell Publishing; 2008:45-54.
3. Kelly DG, Tappenden KA, and Winkler MF. Short bowel syndrome: highlights of patient management, quality of life, and survival. *JPEN J Parenter Enteral Nutr.* 2013.
4. Amiot A, Messing B, Corcos O, Panis Y, and Joly F. Determinants of home parenteral nutrition dependence and survival of 268 patients with non-malignant short bowel syndrome. *Clinical nutrition.* 2013;32(3):368-74.
5. Cisler JJ, and Buchman AL. Intestinal adaptation in short bowel syndrome. *J Investig Med.* 2005;53(8):402-13.
6. Warner BW. The pathogenesis of resection-associated intestinal adaptation. *Cell Mol Gastroenterol Hepatol.* 2016;2(4):429-38.
7. McDuffie LA, Bucher BT, Erwin CR, Wakeman D, White FV, and Warner BW. Intestinal adaptation after small bowel resection in human infants. *J Pediatr Surg.* 2011;46(6):1045-51.
8. Doldi SB. Intestinal adaptation following jejuno-ileal bypass. *Clin Nutr.* 1991;10(3):138-45.
9. Ziegler TR, Fernandez-Estivariz C, Gu LH, Bazargan N, Umeakunne K, Wallace TM, Diaz EE, Rosado KE, Pascal RR, Galloway JR, et al. Distribution of the H+/peptide transporter PepT1 in human intestine: up-regulated expression in the colonic mucosa of patients with short-bowel syndrome. *Am J Clin Nutr.* 2002;75(5):922-30.
10. O'Keefe SJ, Haymond MW, Bennet WM, Oswald B, Nelson DK, and Shorter RG. Long-acting somatostatin analogue therapy and protein metabolism in patients with jejunostomies. *Gastroenterology.* 1994;107(2):379-88.
11. Porus RL. Epithelial hyperplasia following massive small bowel resection in man. *Gastroenterology.* 1965;48(753-7.
12. Schwartz LK, O'Keefe SJ, Fujioka K, Gabe SM, Lamprecht G, Pape UF, Li B, Youssef NN, and Jeppesen PB. Long-term teduglutide for the treatment of patients with intestinal failure associated with short bowel syndrome. *Clin Transl Gastroenterol.* 2016;7(e142.
13. Kinchen J, Chen HH, Parikh K, Antanaviciute A, Jagielowicz M, Fawkner-Corbett D, Ashley N, Cubitt L, Mellado-Gomez E, Attar M, et al. Structural remodeling of the human colonic mesenchyme in inflammatory bowel disease. *Cell.* 2018;175(2):372-86 e17.
14. Santos AJM, Lo YH, Mah AT, and Kuo CJ. The intestinal stem cell niche: homeostasis and adaptations. *Trends in Cell Biology.* 2018.
15. Vishy CE, Swietlicki EA, Gazit V, Amara S, Heslop G, Lu J, Levin MS, and Rubin DC. Epimorphin regulates the intestinal stem cell niche via effects on the stromal microenvironment. *Am J Physiol Gastrointest and Liver Physiol.* 2018;315(2).
16. Shaker A, Swietlicki EA, Wang L, Jiang S, Onal B, Bala S, DeSchryver K, Newberry R, Levin MS, and Rubin DC. Epimorphin deletion protects mice from inflammation-induced colon carcinogenesis and alters stem cell niche myofibroblast secretion. *J Clin Invest.* 2010;120(6):2081-93.
17. Swietlicki EA, Bala S, Lu J, Shaker A, Kularatna G, Levin MS, and Rubin DC. Epimorphin deletion inhibits polyposis in the Apcmin/+ mouse model of colon carcinogenesis via decreased myofibroblast HGF secretion. *Am J Physiol Gastrointest and Liver Physiol.* 2013;305(8):G564-72.
18. Aoki R, Shoshkes-Carmel M, Gao N, Shin S, May CL, Golson ML, Zahm AM, Ray M, Wiser CL, Wright CVE, et al. Foxl1-expressing mesenchymal cells constitute the intestinal stem cell niche. *Cell Mol Gastroenterol and Hepatol.* 2016;2:175-88.
19. Shoshkes-Carmel M, Wang YJ, Wangensteen KJ, Toth B, Kondo A, Massasa EE, Itzkovitz S, and Kaestner KH. Subepithelial telocytes are an important source of Wnts that supports intestinal crypts. *Nature.* 2018;557(7704):242-6.
20. Greicius G, Kabiri Z, Sigmundsson K, Liang C, Bunte R, Singh MK, and Virshup DM. PDGFRalpha(+) pericryptal stromal cells are the critical source of Wnts and RSPO3 for murine intestinal stem cells in vivo. *Proc Natl Acad Sci U S A.* 2018;115(14):E3173-E81.
21. Worthley DL, Churchill M, Compton JT, Tailor Y, Rao M, Si Y, Levin D, Schwartz MG, Uygur A, Hayakawa Y, et al. Gremlin 1 identifies a skeletal stem cell with bone, cartilage, and reticular stromal potential. *Cell.* 2015;160(1-2):269-84.
22. Degirmenci B, Valenta T, Dimitrieva S, Hausmann G, and Basler K. GLI1-expressing mesenchymal cells form the essential Wnt-secreting niche for colon stem cells. *Nature.* 2018;558(7710):449-53.
23. Valenta T, Degirmenci B, Moor Andreas E, Herr P, Zimmerli D, Moor Matthias B, Hausmann G, Cantù C, Aguet M, and Basler K. Wnt Ligands Secreted by Subepithelial Mesenchymal Cells Are Essential for the Survival of Intestinal Stem Cells and Gut Homeostasis. *Cell Reps.* 2016;15(5):911-8.
24. Stzepourginski I, Nigro G, Jacob JM, Dulauroy S, Sansonetti PJ, Eberl G, and Peduto L. CD34+ mesenchymal cells are a major component of the intestinal stem cells niche at homeostasis and after injury. *Proc Natl Acad Sci U S A.* 2017;114(4):E506-E13.
25. Rubin DC, and Levin MS. Mechanisms of intestinal adaptation. *Best Pract Res Clin Gastroenterol.* 2016;30(2):237-48.
26. Yu C, Jiang S, Lu J, Coughlin CC, Wang Y, Swietlicki EA, Wang L, Vietor I, Huber LA, Cikes D, et al. Deletion of Tis7 protects mice from high-fat diet-induced weight gain and blunts the intestinal adaptive response postresection. *J Nutr.* 2010;140(11):1907-14.
27. Greicius G, and Virshup DM. Stromal control of intestinal development and the stem cell niche. *Differentiation.* 2019;108(8-16.

28. Roche KC, Gracz AD, Liu XF, Newton V, Akiyama H, and Magness ST. SOX9 maintains reserve stem cells and preserves radioresistance in mouse small intestine. *Gastroenterology.* 2015;149(6):1553-63 e10.
29. Yan KS, Gevaert O, Zheng GXY, Anchang B, Probert CS, Larkin KA, Davies PS, Cheng ZF, Kaddis JS, Han A, et al. Intestinal enteroendocrine lineage cells possess homeostatic and injury-inducible stem cell activity. *Cell Stem Cell.* 2017;21(1):78-90 e6.
30. Sailaja BS, He XC, and Li L. The regulatory niche of intestinal stem cells. *J Physiol.* 2016;594(17):4827-36.
31. Yan KS, Janda CY, Chang J, Zheng GXY, Larkin KA, Luca VC, Chia LA, Mah AT, Han A, Terry JM, et al. Non-equivalence of Wnt and R-spondin ligands during Lgr5(+) intestinal stem-cell self-renewal. *Nature.* 2017;545(7653):238-42.
32. Kim KA, Kakitani M, Zhao J, Oshima T, Tang T, Binnerts M, Liu Y, Boyle B, Park E, Emtage P, et al. Mitogenic influence of human R-spondin1 on the intestinal epithelium. *Science.* 2005;309(5738):1256-9.
33. Kosinski C, Li VS, Chan AS, Zhang J, Ho C, Tsui WY, Chan TL, Mifflin RC, Powell DW, Yuen ST, et al. Gene expression patterns of human colon tops and basal crypts and BMP antagonists as intestinal stem cell niche factors. *Proc Natl Acad Sci U S A.* 2007;104(39):15418-23.
34. Shaker A, and Rubin DC. Intestinal stem cells and epithelial-mesenchymal interactions in the crypt and stem cell niche. *Transl Res.* 2010;156(3):180-7.
35. Goyal A, Singh R, Swietlicki EA, Levin MS, and Rubin DC. Characterization of rat epimorphin/syntaxin 2 expression suggests a role in crypt-villus morphogenesis. *Am J Physiol Gastrointest Liver Physiol.* 1998;38(1):G114-G24.
36. Wang Y, Wang L, Iordanov H, Swietlicki EA, Zheng Q, Jiang S, Tang Y, Levin MS, and Rubin DC. Epimorphin(-/-) mice have increased intestinal growth, decreased susceptibility to dextran sodium sulfate colitis, and impaired spermatogenesis. *J Clin Invest.* 2006;116(6):1535-46.
37. Marchix J, Goddard G, and Helmrath MA. Host-Gut Microbiota Crosstalk in Intestinal Adaptation. *Cell Mol Gastroenterol Hepatol.* 2018;6(2):149-62.
38. Barker N, van Es JH, Kuipers J, Kujala P, van den Born M, Cozijnsen M, Haegebarth A, Korving J, Begthel H, Peters PJ, et al. Identification of stem cells in small intestine and colon by marker gene Lgr5. *Nature.* 2007;449(7165):1003-7.
39. Sangiorgi E, and Capecchi MR. Bmi1 is expressed in vivo in intestinal stem cells. *Nat Genet.* 2008;40(7):915-20.
40. Kraiczy J, Nayak KM, Howell KJ, Ross A, Forbester J, Salvestrini C, Mustata R, Perkins S, Andersson-Rolf A, Leenen E, et al. DNA methylation defines regional identity of human intestinal epithelial organoids and undergoes dynamic changes during development. *Gut.* 2019;68(1):49-61.
41. Suzuki K, Murano T, Shimizu H, Ito G, Nakata T, Fujii S, Ishibashi F, Kawamoto A, Anzai S, Kuno R, et al. Single cell analysis of Crohn's disease patient-derived small intestinal organoids reveals disease activity-dependent modification of stem cell properties. *J Gastroenterol.* 2018;53(9):1035-47.
42. Dotti I, Mora-Buch R, Ferrer-Picon E, Planell N, Jung P, Masamunt MC, Leal RF, Martin de Carpi J, Llach J, Ordas I, et al. Alterations in the epithelial stem cell compartment could contribute to permanent changes in the mucosa of patients with ulcerative colitis. *Gut.* 2017;66(12):2069-79.
43. He XC, Zhang J, Tong WG, Tawfik O, Ross J, Scoville DH, Tian Q, Zeng X, He X, Wiedemann LM, et al. BMP signaling inhibits intestinal stem cell self-renewal through suppression of Wnt-beta-catenin signaling. *Nat Genet.* 2004;36(10):1117-21.
44. Sato T, Vries RG, Snippert HJ, van de Wetering M, Barker N, Stange DE, van Es JH, Abo A, Kujala P, Peters PJ, et al. Single Lgr5 stem cells build crypt-villus structures in vitro without a mesenchymal niche. *Nature.* 2009;459(7244):262-5.
45. Zhang Y, and Que J. BMP signaling in development, stem cells, and diseases of the gastrointestinal tract. *Annu Rev Physiol.* 2020;82:9.1-9.23.
46. Bernal NP, Stehr W, Zhang Y, Profitt S, Erwin CR, and Warner BW. Evidence for active Wnt signaling during postresection intestinal adaptation. *J Pediatr Surg.* 2005;40(6):1025-9; discussion 9.
47. Sukhotnik I, Roitburt A, Pollak Y, Dorfman T, Matter I, Mogilner JG, Bejar J, and Coran AG. Wnt/beta-catenin signaling cascade down-regulation following massive small bowel resection in a rat. *Pediatr Surg Int.* 2014;30(2):173-80.
48. Stern LE, Erwin CR, O'Brien DP, Huang F, and Warner BW. Epidermal growth factor is critical for intestinal adaptation following small bowel resection. *Micros Res Tech.* 2000;51(2):138-48.
49. Sato T, Stange DE, Ferrante M, Vries RG, Van Es JH, Van den Brink S, Van Houdt WJ, Pronk A, Van Gorp J, Siersema PD, et al. Long-term expansion of epithelial organoids from human colon, adenoma, adenocarcinoma, and Barrett's epithelium. *Gastroenterology.* 2011;141(5):1762-72.
50. Eyden B. The myofibroblast: phenotypic characterization as a prerequisite to understanding its functions in translational medicine. *J Cell Mol Med.* 2008;12(1):22-37.
51. Rao X, Huang X, Zhou Z, and Lin X. An improvement of the 2^(-delta delta CT) method for quantitative real-time polymerase chain reaction data analysis. *Biostat Bioinforma Biomath.* 2013;3(3):71-85.
52. Yang FQ, Yang FP, Li W, Liu M, Wang GC, Che JP, Huang JH, and Zheng JH. Foxl1 inhibits tumor invasion and predicts outcome in human renal cancer. *Int J Clin Exp Path.* 2014;7(1):110-22.

Figure legends

Figure 1: **Increased crypt cell proliferation in small bowel biopsies from short bowel syndrome patients compared to normal control subjects**. A. Increased *KI67 (*p=0.027*) CD44* (*p=0.012*)* and *EGFR* (*p=0.011) mRNA levels in SBS vs normal small bowel, quantified by qRT-PCR. B-E. Representative images of immunohistohemical analysis of KI67 expression (brown cells) in normal (B,C) and SBS (D,E) small bowel. Arrows depict representative full length intestinal crypts. F. Increased *LGR5* mRNA levels (**p=0.007) in SBS vs control small bowel. MRNA levels of +4 position stem cell markers *SOX9* and *BMI1* are unchanged. SBS; n=9-12; normal; n=16-24. Data are means ± SEM. Statistical analysis by Student's t test.

Figure 2. *LGR5* mRNA expression is increased in the crypt base of SBS compared to control ileum. A. *In situ* hybridization by RNAscope to detect *LGR5* mRNA (small green dots, white arrows), on sections of normal ileum (top panels) and SBS ileum (bottom panels). Slides are counterstained with DAPI for nuclei (blue). Orange arrows denote lamina propria cells which have intrinsic auto fluorescence leading to artifact. B. Quantitation of the number of *LGR5*+ dots per crypt from sections of normal (n=8) and SBS (n=6) ileal biopsies (*p=0.034). Data are means ± SEM. Statistical analysis by Student's t test.

Figure 3: Stem cell expansion in small intestine from patients with short bowel syndrome. Stem cells isolated from small bowel biopsies from patients with short bowel syndrome and from normal controls were plated for stem cell enteroid initiation assays as per Methods. The number of enteroids per well and enteroid size (cross-sectional area) were quantified using the Cytation 3 plate reader. A. Average number of stem cell derived enteroids from biopsies from normal patients (n=12) and short bowel syndrome (SBS) patients (n=7) grown in Matrigel for seven days. *p = 0.0178. Twenty wells were analyzed for each patient and experiments were repeated at least twice. B. Average cross-sectional area of SBS (n=7) vs normal (n=12) patient stem cell derived enteroids. All data are means ± SEM. Statistical analysis by Student's t test. C. Photomicrographs of normal (left panel) and SBS (right panel) stem cell derived enteroids. Bar = 50 microns, imaged by Zeiss Axiophot with Apoptome 2 microscopy**.**

Figure 4: ***WNT* signaling pathway component gene expression in SBS vs. control small intestinal biopsies**. Relative mRNA levels were measured by qRT-PCR. A. *WNT* target gene analysis shows that *AXIN2* mRNA expression showed a trend to be decreased in SBS vs control ileum, p= 0.054, but other target gene mRNA levels are unchanged. B. *WNT5A* and *R-SPONDIN1 and 2* mRNA levels are increased in SBS. Normal; n=13-24; SBS; n=7-12. *WNT5A*, *p=0.049; *R-SPONDIN* 1 *p=0.048; *R-SPONDIN2* **p=0.01. Data are means ± SEM. Statistical analysis is by Student's t test.

Figure 5: BMP signaling pathway mRNA expression in SBS vs. normal small bowel biopsies. A. Total RNA was isolated from normal (n=12-23) and SBS (n=6-10) small bowel biopsies and mRNA levels were quantified by qRT-PCR. *BMP4* *p=0.009; data are means ± SEM. Statistical analysis by Student's t test. B. Immunoblot to detect P-SMAD1,5,8 expression in SBS compared to normal ileum. First lane (left), molecular weight markers; second and third lanes, SBS, n= 2 patients pooled per lane) and fourth lane, normal (n= 2 patients pooled). C. Quantitation of relative P-SMAD1,5,8 protein expression was performed by optical densitometric (LI-COR) analysis of P-SMAD1,5,8 and β-actin bands. P-SMAD1,5,8 expression was normalized to β-actin and SBS P-SMAD1,5,8 expression was calculated relative to normal ileal expression.

Figure 6. Mesenchymal cell marker gene expression analyses. Stem cell niche mesenchymal cell marker gene expression by qRT-PCR analysis of mRNA from normal (n=12-24) and SBS (n=9-13) small bowel biopsies. A. A subset of mesenchymal markers including myofibroblast markers (*epimorphin, A-SMA, vimentin),* and *PDGFRα* and *FOXL1* exhibited increased mRNA levels in SBS vs normal small bowel. *Epimorphin* *p=0.042; *SMA* *p=0.024; *vimentin* **p=0.012; *FOXL1* *p=0.049; *PDGFRα* *p=0.009; *CD34* *p=0.025. Data are means ± SEM. Statistical analysis Student's t test. B. PDGFRα+ cells (brown stained cells) in normal (upper panel) and SBS (lower panel) ileal biopsies detected by immunohistochemical analysis, using a mouse anti-human PDGFRα antibody. Black arrows on high power views (right panels) show PDGFRα+ cells subjacent to the villi. Red arrows on low power view (left panels) depict the crypts. Green arrows (middle panels) show the crypt-villus junction C. The number of crypt and villus associated PDGRα+ cells was quantified in SBS patient crypts (n=8) and villi (n=9) and normal patient crypts (n=11) and villi (n=11). Each

data point represents the average percentage of positive cells per patient. Only intact villi and crypts on each histologic section were analyzed. *p= 0.031. Data are means ± SEM. Statistical analysis by Student's t test.

Figure 7: SBS ISEMFs increase surface area of co-cultured ileal SBS enteroids. Normal enteroids (n=9 patients) and SBS enteroids (n= 6 patients) were co-cultured for seven days with normal (n= 4 subjects) or SBS (n=4 patients) ISEMFs. Enteroid cross-sectional area (A) and the number of enteroids (cell count, B) were quantified by Cytation 3. A. SBS enteroid size *** p=0.0006; B. Normal enteroid cell count **p=0.0068; SBS enteroids= cell count, NS. Data are means ±SEM. Statistical analysis by Student's t test. C. Images of ISEMF-enteroid co-cultures by Zeiss Axiophot microscope with Apotome 2 attachment. Scale bar = 50 microns.

Figure 8: Mesenchymal marker and BMP signaling pathway gene expression in normal and SBS ISEMFs. A. SBS ISEMFs have increased smooth muscle- α-actin (α-SMA *p=0.0109) but reduced *epimorphin* mRNA expression (*p=0.0264) compared to normal ISEMFS. Data are mean +/- SEM. Statistical analysis by Student's t test. There was no change in *FOXL1* or *PDGFRα* mRNA expression. B. Immunohistochemical analysis of human normal and SBS ISEMFs shows expression of myofibroblast marker genes *α-SMA* and *vimentin*. C. BMP4 signaling pathway gene expression in SBS ISEMFs. ISEMFs from normal and SBS patient biopsies were isolated as per Methods. BMP4 mRNA is reduced in SBS *p=0.0528. SBS, n=4; normal, n= 7-8). Data are means ± SEM. Statistical analysis by Student's t test.

Figure 9: BMP4 reverses the effects of SBS ISEMFs on co-cultured SBS enteroid growth. A. SBS enteroids were co-cultured with normal human ISEMFs or with SBS ISEMFs in enteroid growth conditioned media (CM), in CM without noggin (-noggin), or in CM without noggin but with BMP4 (BMP4 (25 ng/ml, ± noggin). BMP4 reversed the increase in enteroid size induced by co-culture with SBS ISEMFs. ** p=0.0064; *p=0.04. B. Normal enteroids were co-cultured with normal or SBS ISEMFs in CM, in CM without noggin, or in CM without noggin but with BMP4. No change in enteroid size was noted. C. Normal enteroids were co-cultured with normal ISEMFs without noggin, with normal ISEMFs without noggin but with BMP4, with SBS

ISEMFs without noggin or with SBS ISEMFs without noggin plus BMP4, and cell count was measured. A significant decrease in enteroid cell count was observed in co-cultures with SBS ISEMFs *p=0.01 normal enteroids with normal ISEMFS vs normal enteroids with SBS ISEMFs; with BMP4; this decrease was not reversed by treatment with BMP4. SBS enteroids, n=4 patients; normal enteroids, n=5-7 patients; normal ISEMFs, n=3 patients; SBS ISEMFs, n=4 patients. Data are mean +/- SEM. Statistical analysis by Student's t test.

Table 1: Demographic Data for SBS patients

Number of patients	17
Age, years (±SD)*	59.64 ± 11.12
Gender	
Male	7
Female	10
Cause of SBS	
Radiation enteritis	3
Crohn's disease	6
Ischemia	4
Fistula	1
Trauma	1
Adhesions	2
On/Off TPN	
On TPN	11
Off TPN	6
Colon/No colon	
Remnant colon (>50%) in continuity	9
Remnant colon (<50%) in continuity	1
Small bowel ostomy	7

* SD= standard deviation

Table 2: PCR primer sequences

Human Gene	Forward Primer	Reverse Primer
h18s	*5'-GTAACCCGTTGAACCCCATT-3'*	*5'-CCATCCAATCGGTAGTAGCG-3'*
hGAPDH	*5'-TGCACCACCAACTGCTTAGC-3'*	*5'-GGCATGGACTGTGGTCATGAG-3'*
hEPIMORPHIN/SYNTAXIN2	*5'-GGAACCGAACTTCAGTGGAT-3'*	*5'-GTGAAGATGGATGGCTTCCC-3'*
hα-SMA	*5'-CCGACCGAATGCAGAAGGA-3'*	*5'-ACAGAGTATTTGCGCTCCGAA-3'*
hVIMENTIN1	*5'-CACGAAGAGGAAATCCGGAGC-3'*	*5'-CAGGGCGTCATTGTTCCG-3'*
hFOXL1 (52)	*5'-TTATTTGGCGGACAGTGACA-3'*	*5'-ACACGGCATCAATCTTTTCC-3'*
hPDGFRα	*5'-GGAAGGTGGTTGAAGGAACA-3'*	*5'-CCAGAGCAGAATGCCATAAGA-3'*
hLGR5	*5'-ACAAGGGAGACCTGGAGAATA-3'*	*5'-GTGATGCTGGAGCTGGTAAA-3'*
hEGFR	*5'-GCTGGATGATAGACGCAGATAG-3'*	*5'- TGGGAACGGACTGGTTTATG-3'*
hCD44	*5'-AAGACATCTAACCCAGCA-3'*	*5'-GGTAGCAGGGATTCTGTC-3'*
hCD34	*5-ACACCTAGTACCCTTGGAAGT-3'*	*5'-GCCTTGATGTCACTTAGGATAGG-3'*
hGP38(PDPN)	*5'-GTCAGCTCTGCTCTTCGTTT-3'*	*5'-GTGTGTCTCCATCCACTTTCTC-3'*
hBMI1	*5'-GTTCACAAGACCAGACCACTAC-3'*	*5'-CTGCTGGGCATCGTAAGTATC-3'*
hBMP2	*5' – ATGGATTCGTGGTGGAAGTG-3'*	*5'-GAGTTCAGATGATCAGCCAGAG-3'*
hBMP4	*5'GATCCACAGCACTGGTCTTG-3'*	*5'-GGGATGCTGCTGAGGTTAAA-3'*
hBMP7	*5'- GTAAGAAGCACGAGCTGTATGT-3'*	*5'-GTTGGAGCTGTCATCGAAGTAG-3'*
hGREMLIN1	*5'-ATGTGACGGAGCGCAAATAC-3'*	*5'-TGGATATGCAACGACACTGC-3'*
hNOGGIN	*5'-GGAGGAAGTTACAGATGTGGCTGT-3'*	*5'-CACTCGGAAATGATGGGGTACTG-3'*
hCHORDIN	*5'-CAGGAGTGGGGGACTAACC-3'*	*5'-CAGCACCTCAGCAAAGCCT-3'*
hFOLLISTATIN	*5'-CGGATCTTGCAACTYFAATCT-3'*	*5'-TCAAAGCCCTCTGATACAGC-3'*
hWNT2b	*5'-GGCTGCTACCGCTTCTATTT-3'*	*5'-CTCTACAGGTACCCTTCCTCTT-3'*
hWNT4	*5'-CTTCGTGTACGCCATCTCTTC-3'*	*5'-CTCAGTGGCACCATCAAACT-3'*
hWNT5a	*5'-CACCAGAGCAGACAACCTATTT-3'*	*5'-CTTCAACCCAACACGCATTTC-3'*
hAXIN2	*5'-GAAGCTCTTGTGAACTGTCT-3'*	*5'-TTCAGGCTTTTCTTATCTCAG-3'*
hSOX9	*5'-GGAGGAAGTCGGTGAAGAAC-3'*	*5'-CTGTAGTGTGGGAGGTTGAAG-3'*
hDKK1	*5'-TTCTGTTTGTCTCCGGTCATC-3'*	*5'-TACTGGCTTGATGGTGATCTTT-3'*
hβ-CATENIN	*5'-ACAGCACCTTCAGCACTCT-3'*	*5'-AAGTTCTTGGCTATTACGACA-3'*
hCYCLIND1	*5'-GTCTTCCCGCTGGCCATGAACTAC-3'*	*5'-GGAAGCGTGTGAGGCGGTAGTAGG-3'*
hC-MYC	*5'-CCTACCCTCTCAACGACAGC-3'*	*5'- CTCTGACCTTTTGCCAGGAG-3'*
hR-SPONDIN1	*5'-TCACCCAAGCTGTTCATCC-3'*	*5'-AGACCACTCGCTCATTTCAC-3'*
hR-SPONDIN2	*5'-GCAGTAAGCGAGCTAGTTATGTA-3'*	*5'-ATCAAAGCAACGGCCTCTAT-3'*
hR-SPONDIN3	*5'-TGGAGGCCAACAACCATACT-3'*	*5'-GTTCTCCCTTCTGACACTTCTT-3'*
hKI-67	*5'-GAAGAGGCCCAATCACTAGAAG-3'*	*5'-CTGCACTGGAGTTCCCATAAA-3'*
hGLI3	*5'ACTACCACCCTCCTCATCTT - -3'*	*5'CTGTGCAAGGAGCGGATATAG- -3'*
hGLI1	*5'-CTACATCAACTCCGGCCAATAG-3'*	*5'-GGTTGGGAGGTAAGGATCAAAG-3'*

Supplemental Table 1: Demographics of short bowel syndrome patients

Gender	*Age (years)*	*Race*	*Cause of SBS*	*On/Off TPN*	*Colon present (yes/no)*	*SBS duration*
F	76	White	Radiation enteritis	On TPN	Yes (<50%)	30y
F	44	White	Crohn's	On TPN	No	6m
F	66	White	Crohn's	Off TPN	No	11m
F	64	White	Perforation	Off TPN	No	12m
M	69	White	Ischemia	On TPN	Yes	10y
F	52	White	Fistula	On TPN	Yes	12m
M	72	White	Crohn's	On TPN	No	21m
F	71	White	Radiation enteritis	On TPN	Yes	4y
M	37	White	Ischemia	Off TPN	Yes	4y
M	65	White	Trauma	On TPN	Yes	2y
F	60	White	Adhesions	On TPN	Yes	10y
F	47	White	Ischemia	On TPN	Yes	10m
F	61	White	Adhesions	On TPN	Yes	20m
M	68	White	Crohn's	Off TPN	No	4y
M	53	White	Crohn's	Off TPN	No	6y
M	47	White	Crohn's	Off TPN	No	10y
F	62	White	Radiation enteritis	On TPN	Yes	1y

N=17 patients; y=years, m=months

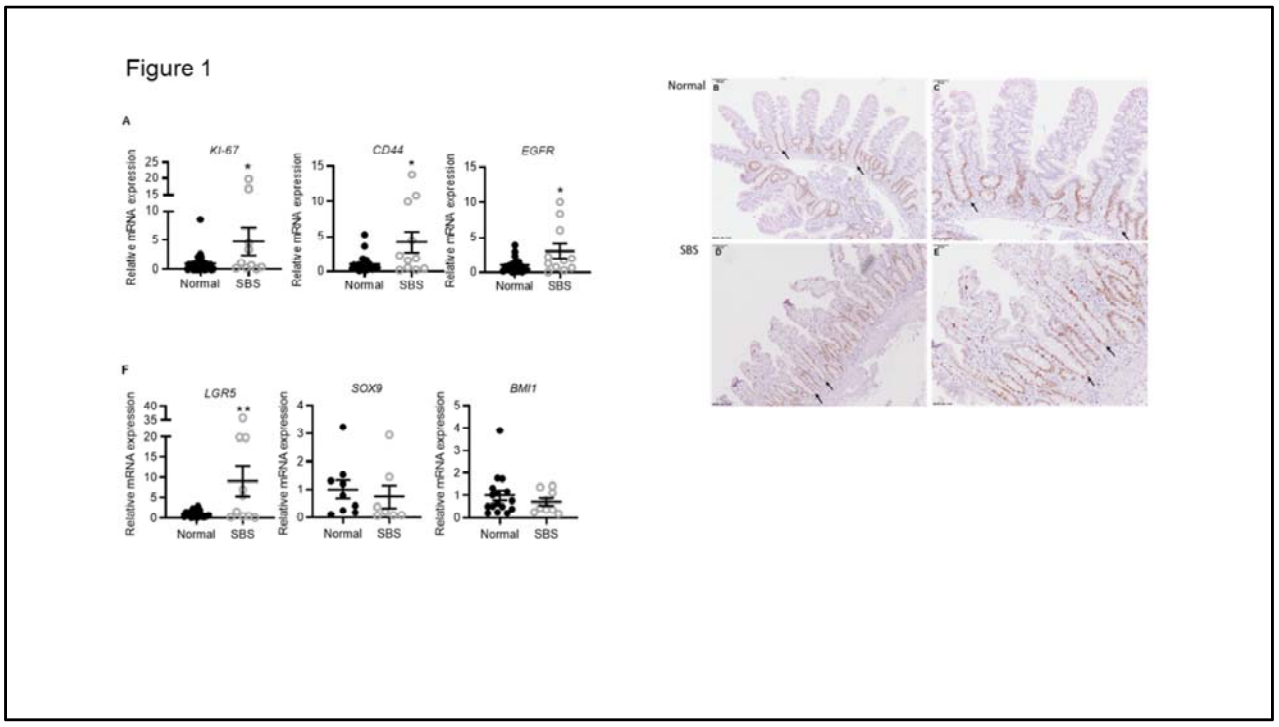

Figure 1: **Increased crypt cell proliferation in small bowel biopsies from short bowel syndrome patients compared to normal control subjects**. A. Increased *KI67 (*p=0.027*) CD44* (*p=0.012*)* and *EGFR* (*p=0.011) mRNA levels in SBS vs normal small bowel, quantified by qRT-PCR. B-E. Representative images of immunohistohemical analysis of KI67 expression (brown cells) in normal (B,C) and SBS (D,E) small bowel. Arrows depict representative full length intestinal crypts. F. Increased *LGR5* mRNA levels (**p=0.007) in SBS vs control small bowel. MRNA levels of +4 position stem cell markers *SOX9* and *BMI1* are unchanged. SBS; n=9-12; normal; n=16-24. Data are mean ± SEM. Statistical analysis by Student's t test.

Figure 2

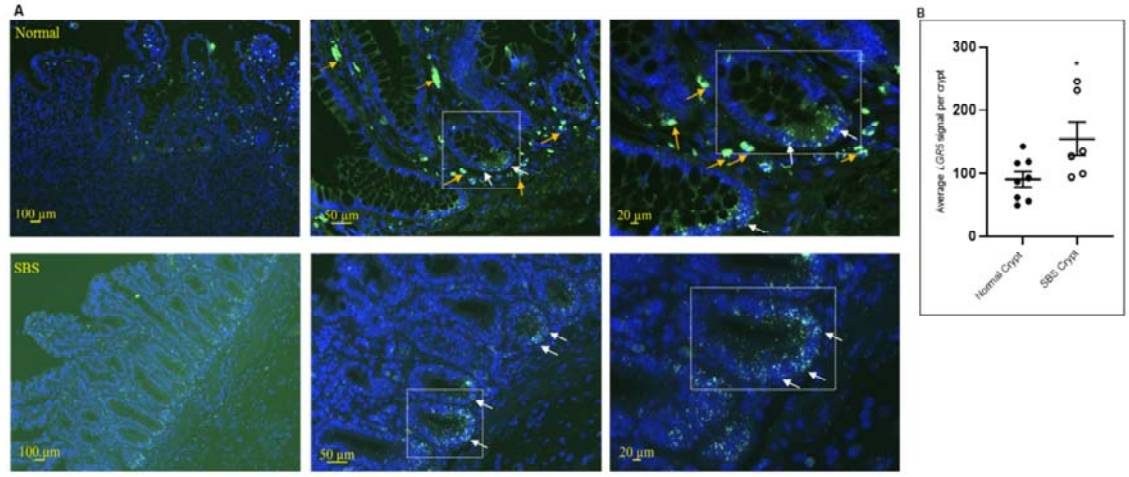

Figure 2. *LGR5* mRNA expression is increased in the crypt base of SBS compared to control ileum. A. *In situ* hybridization by RNAscope to detect *LGR5* mRNA (small green dots, white arrows), on sections of normal ileum (top panels) and SBS ileum (bottom panels). Slides are counterstained with DAPI for nuclei (blue). Orange arrows denote lamina propria cells which have intrinsic autofluorescence leading to artifact. B. Quantitation of the number of *LGR5*+ dots per crypt from sections of normal (n=8) and SBS (n=6) ileal biopsies (*p=0.034). Data are means ± SEM. Statistical analysis by Student's t test.

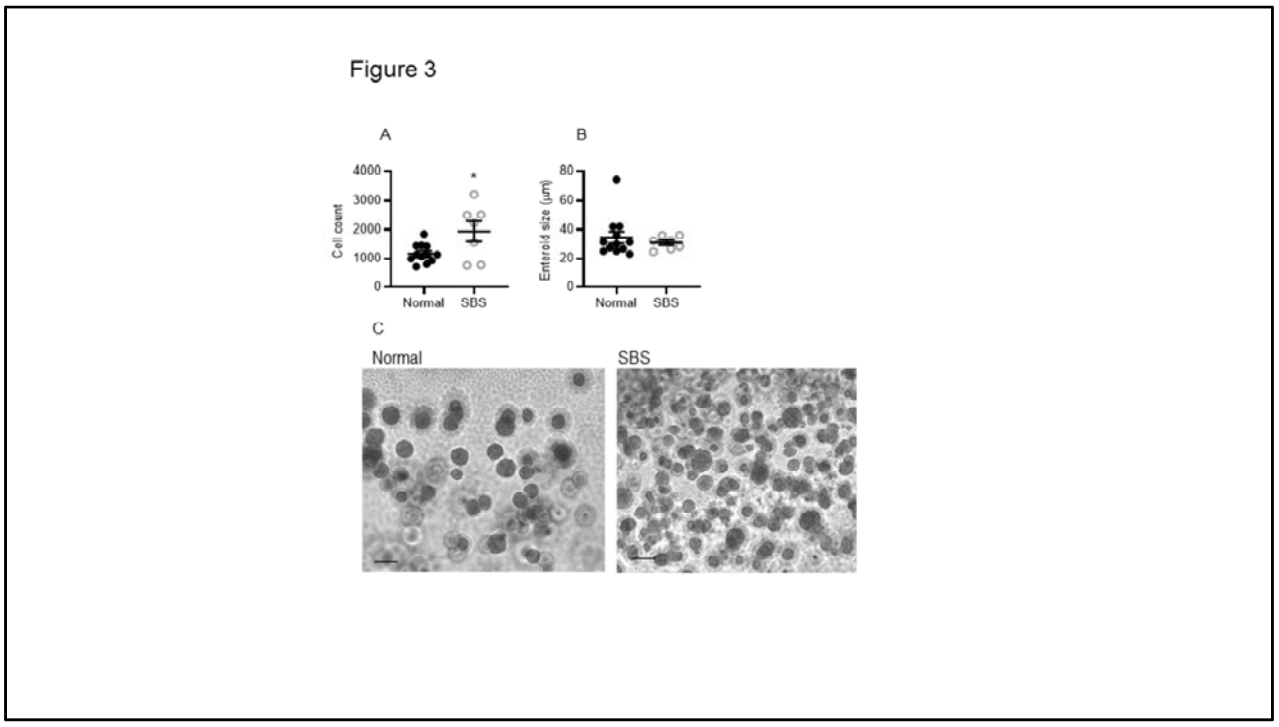

Figure 3: Stem cell expansion in small intestine from patients with short bowel syndrome. Stem cells isolated from small bowel biopsies from patients with short bowel syndrome and from normal controls were plated for stem cell enteroid initiation assays as per Methods. The number of enteroids per well and enteroid size (cross-sectional area) were quantified using the Cytation 3 plate reader. A. Average number of stem cell derived enteroids from biopsies from normal patients (n=12) and short bowel syndrome (SBS) patients (n=7) grown in Matrigel for seven days. *p = 0.0178. Twenty wells were analyzed for each patient and experiments were repeated at least twice. B. Average cross-sectional area of SBS (n=7) vs normal (n=12) patient stem cell derived enteroids. All data are means +/- SEM. Statistical analysis by Student's t test. C. Photomicrographs of normal (left panel) and SBS (right panel) stem cell derived enteroids. Bar = 50 microns, imaged by Zeiss Axiophot with Apoptome 2 microscopy.

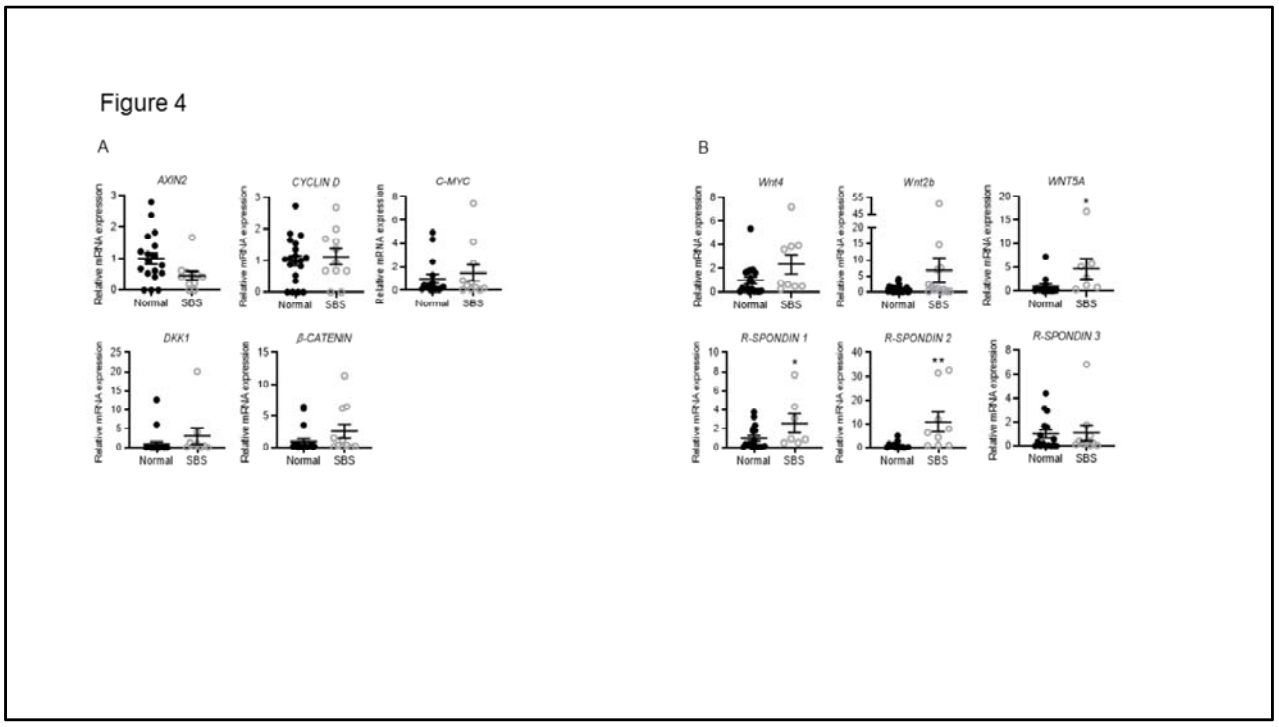

Figure 4: ***WNT* signaling pathway component gene expression in SBS vs. control small intestinal biopsies**. Relative mRNA levels were measured by qRT-PCR. A. *WNT* target gene analysis shows that *AXIN2* mRNA expression showed a trend to be decreased in SBS vs control ileum (p=0.054), but other target gene mRNA levels are unchanged. B. *WNT5A* and *R-SPONDIN1 and 2* mRNA levels are increased in SBS. Normal; n=13-24; SBS; n=7-12. *WNT5A*, *p0.049; *R-SPONDIN* 1 *p=0.048; *R-SPONDIN2* **p=0.01; data are means +/- SEM. Statistical analysis by Student's t test.

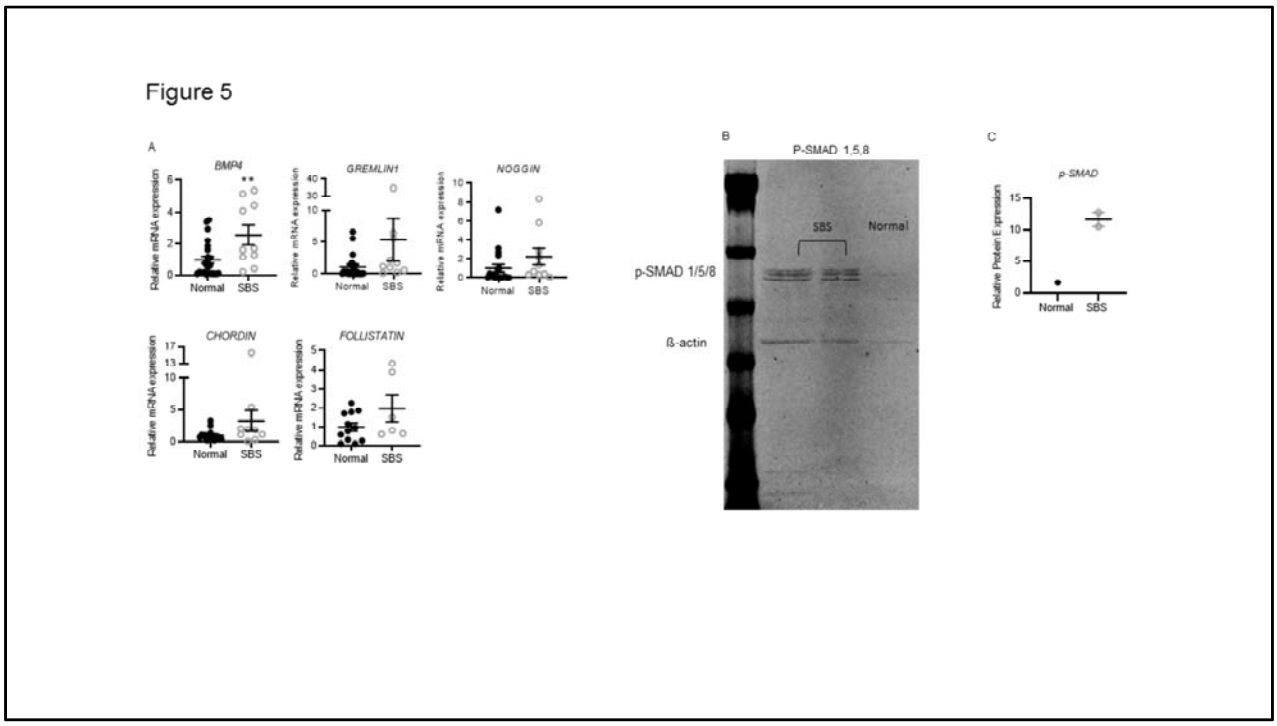

Figure 5: BMP signaling pathway mRNA expression in SBS vs. normal small bowel biopsies. A. Total RNA was isolated from normal (n=12-23) and SBS (n=6-10) small bowel biopsies and mRNA levels were quantified by qRT-PCR. *BMP4* *p=0.009; data are means +/- SEM. Statistical analysis by Student's t test. B. Immunoblot to detect P-SMAD 1,5,8 expression in SBS compared to normal ileum. First lane (left), molecular weight markers; second and third lanes, SBS, n= 2 patients pooled per lane) and fourth lane, normal (n= 2 patients pooled). C. Quantitation of relative P-SMAD1,5,8 protein expression was performed by densitometric analysis of P-SMAD 1,5,8 and β-actin bands. P-SMAD1,5,8 expression was normalized to β-actin and SBS P-SMAD1,5,8 expression was calculated relative to normal ileal expression.

Figure 6

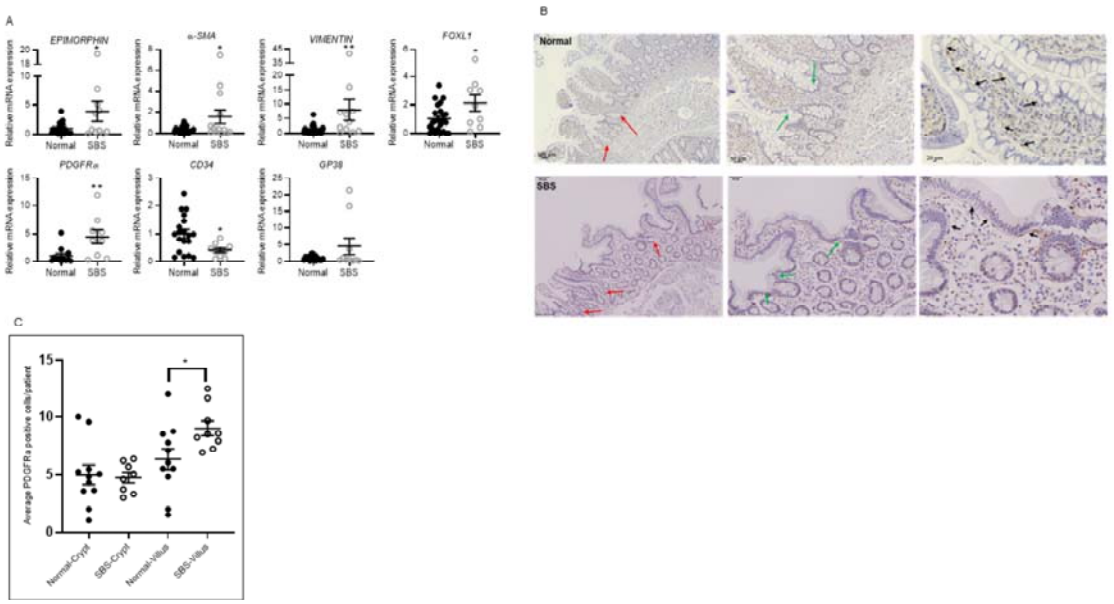

Figure 6. Mesenchymal cell marker gene expression analyses. Stem cell niche mesenchymal cell marker gene expression by qRT-PCR analysis of mRNA from normal (n=12-24) and SBS (n=9-13) small bowel biopsies. A. A subset of mesenchymal markers including myofibroblast markers (*EPIMORPHIN, A-SMA, VIMENTIN),* and *PDGFRα* and *FOXL1* exhibited increased mRNA levels in SBS vs normal small bowel. EPIMORPHIN *p=0.042; SMA *p=0.024; VIMENTIN **p=0.012; FOXL1 *p=0.049; PDGFRα *p=0.009; CD34 *p0.025. Data are means +/- SEM. Statistical analysis by Student's t test. B. PDGFRα+ cells (brown stained cells) in normal (upper panel) and SBS (lower panel) ileal biopsies detected by immunohistochemical analysis, using a mouse anti-human PDGFRα antibody. Black arrows on high power views (right panels) show PDGFRa+ cells subjacent to the villi. Red arrows on low power view (left panels) depict the crypts. Green arrows (middle panels) show the crypt-villus junction C. The number of crypt and villus associated PDGRα+ cells was quantified in SBS patient crypts (n=8) and villi (n=9) and normal patient crypts (n=11) and villi (n=11). Each data point represents the average percentage of positive cells per patient. Only intact villi and crypts on each histologic section were analyzed. *p= 0.031. Data are means +/- SEM. Statistical analysis by Student's t test.

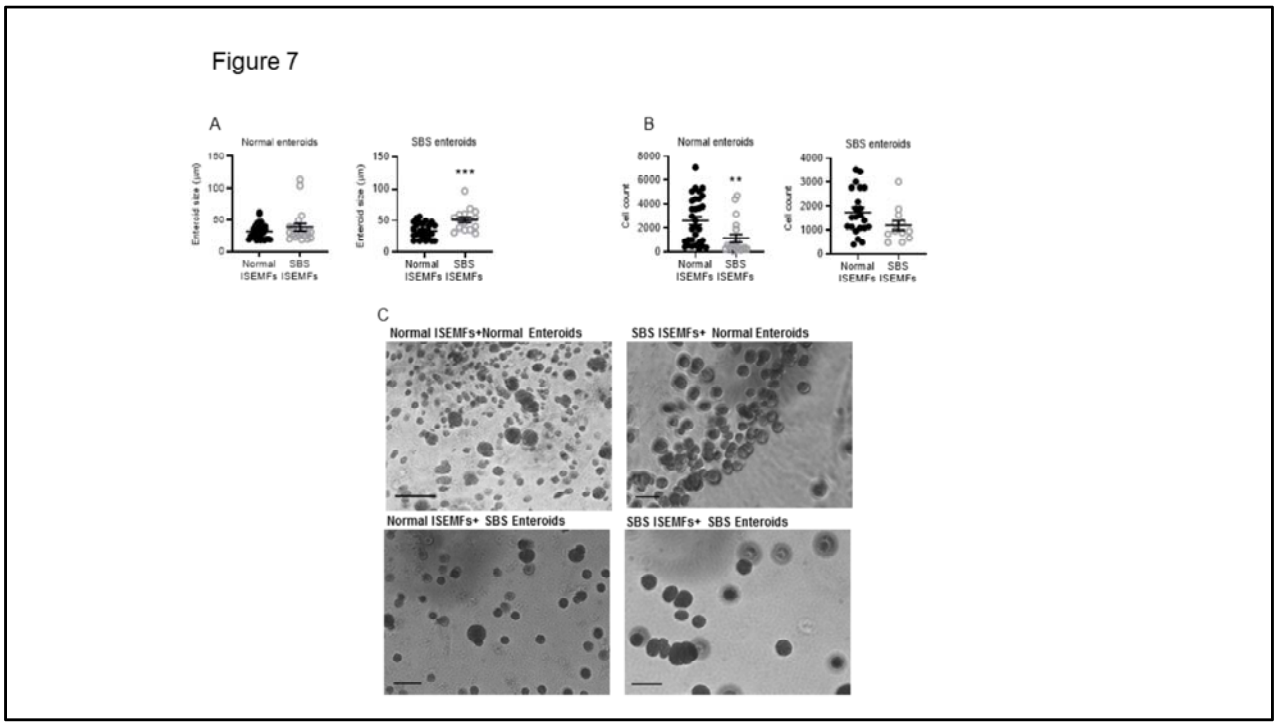

Figure 7: SBS ISEMFs increase surface area of co-cultured ileal SBS enteroids. Normal enteroids (n=9 patients) and SBS enteroids (n= 6 patients) were co-cultured for seven days with normal (n= 4 subjects) or SBS (n=4 patients) ISEMFs. Enteroid cross-sectional area (A) and the number of enteroids (cell count, B) were quantified by Cytation 3. A. SBS enteroid size *** p=0.0006; B. Normal enteroid cell count **p=0.0068; SBS enteroid cell count, NS. Data are means +/- SEM. Statistical analysis by Student's t test. C. Images of ISEMF-enteroid co-cultures by Zeiss Axiophot microscope with Apotome 2 attachment. Bar = 50 microns.

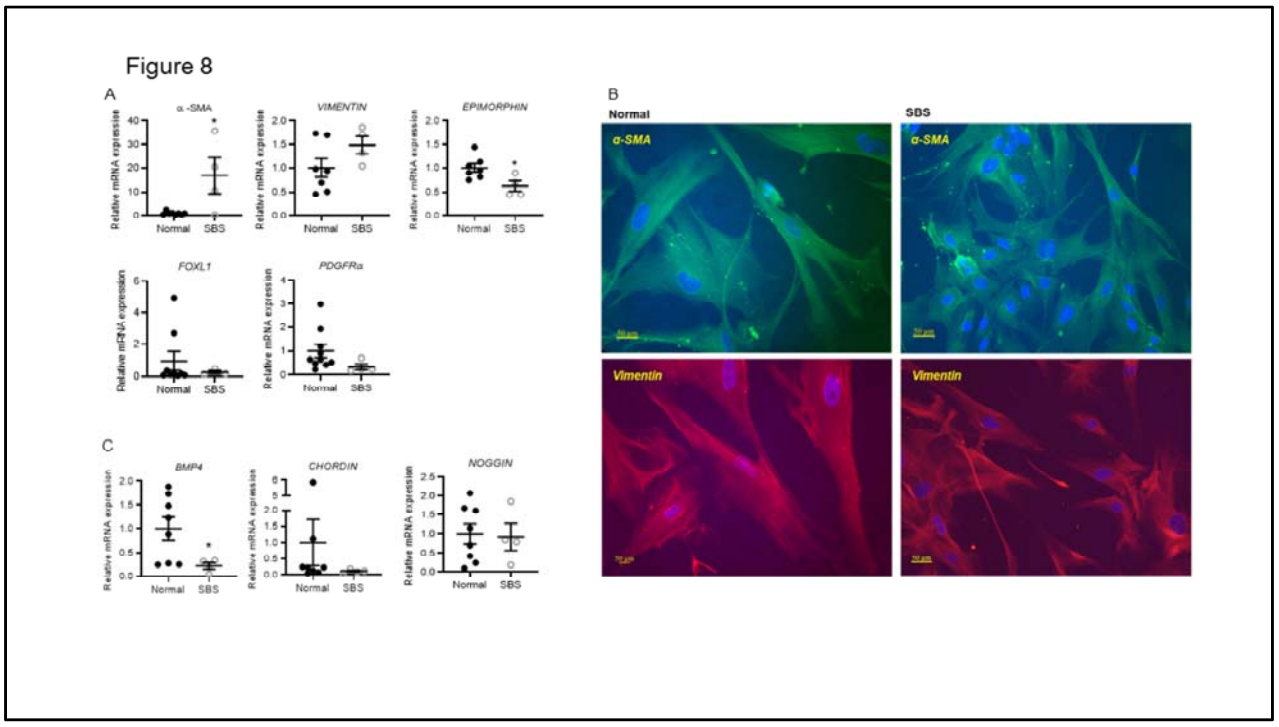

Figure 8: Mesenchymal marker and BMP signaling pathway gene expression in normal and SBS ISEMFs. A. SBS ISEMFs have increased smooth muscle- α-actin (α-SMA *p=0.0109) but reduced *EPIMORPHIN* mRNA expression (*p=0.0264) compared to normal ISEMFS. Data are mean +/- SEM, Student's t test. There was no change in *FOXL1* or *PDGFRα* mRNA expression. B. Immunohistochemical analysis of human normal and SBS ISEMFs shows expression of myofibroblast marker genes *α-SMA* and *VIMENTIN*. C. BMP4 signaling pathway gene expression in SBS ISEMFs. ISEMFs from normal and SBS patient biopsies were isolated as per Methods. BMP4 mRNA is reduced in SBS *p=0.0528. SBS, n=4; normal, n= 7-8). Data are means +/- SEM. Statistical analysis by Student's t test.

Figure 9

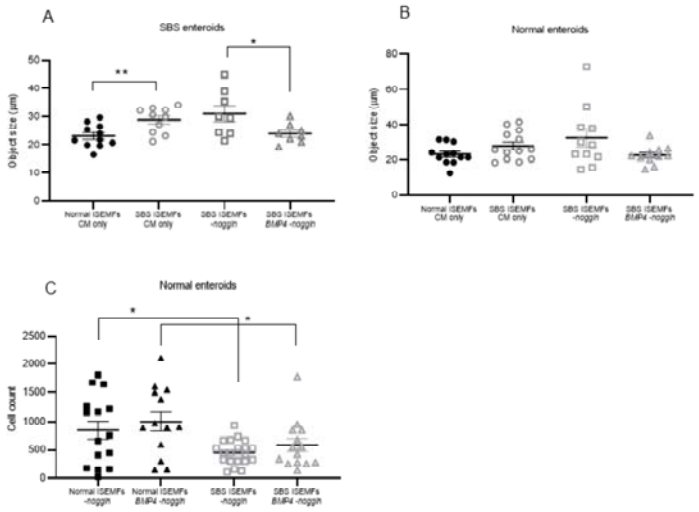

Figure 9: BMP4 reverses the effects of SBS ISEMFs on co-cultured SBS enteroid growth. A. SBS enteroids were co-cultured with normal human ISEMFs or with SBS ISEMFs in enteroid growth conditioned media (CM), in CM without noggin (-noggin), or in CM without noggin but with BMP4 (BMP4 (25 ng/ml, ± noggin). BMP4 reversed the increase in enteroid size induced by co-culture with SBS ISEMFs. ** p=0.0064; *p=0.04. B. Normal enteroids were co-cultured with normal or SBS ISEMFs in CM, in CM without noggin, or in CM without noggin but with BMP4. No change in enteroid size was noted. C. Normal enteroids were co-cultured with normal ISEMFs without noggin, with normal ISEMFs without noggin but with BMP4, with SBS ISEMFs without noggin or with SBS ISEMFs without noggin plus BMP4, and cell count was measured. A significant decrease in enteroid cell count was observed in co-cultures with SBS ISEMFs *p=0.01 normal enteroids with normal ISEMFS vs normal enteroids with SBS ISEMFs; with BMP4 ; this decrease was not reversed by treatment with BMP4. SBS enteroids, n=4 patients; normal enteroids, n=5-7 patients; normal ISEMFs, n=3 patients; SBS ISEMFs, n=4 patients. Data are mean +/- SEM. Statistical analysis by Student's t test.